NTNU
Norwegian University of
Science and Technology

Analysis of electromagnetic behavior of Permanent Magnetized (PM) electrical machines in fault modes

Muhammad Usman Hassan

Wind Energy
Submission date: August 2017
Supervisor: Robert Nilssen, IEL
Co-supervisor: Astrid Røkke, Rolls Royce Marine AS

Norwegian University of Science and Technology
Department of Electric Power Engineering

THESIS REPORT, EUROPEAN WIND ENRGY MASTER, ELECTRICAL POWER SYSTEM

Analysis of Electromagnetic Behavior of Permanent Magnetized Electrical Machines in Fault Modes

by

Muhammad Usman Hassan

in partial fulfillment of the requirements for the degrees of

MSc in Electrical Engineering at Delft University of Technology &
MSc-Technology in Wind Energy at Norwegian University of Science and Technology,

under the European Wind Energy Masters programme.
To be publicly defended on

Friday 25th August 2017 at NTNU

Supervisor :	Prof. R. Nilssen	NTNU
	Dr. ir. H. Polinder	TU Delft
Co-Supervisor :	Dr. A. Røkke	RR
Thesis Committee :	Prof. R. Nilssen	NTNU
	Dr. ir. H. Polinder	TU Delft
	Prof. J. Dong	TU Delft
	Dr. A. Røkke	RR

To my sister,
Ayesha Hassan

Abstract

Over the years, the use of PM machines has been increasing in the offshore wind industry and marine industry. The industries thrive on efficient function of the PM machines. These machines are prone to electro-mechanical faults due to environmental conditions and maintenance. Out of all these faults, stator internal faults are concerning as they can lead to insulation failures which may take around 30 seconds to expand and lead to a fire on ships, or on wind turbines. These type of faults develop gradually, which gives the opportunity to control the fault currents before they reach dangerous levels. Rolls Royce Marine AS is also working to tackle this problem for their hybrid propulsion shaft generator. DNVGL requires the generator to be made electrically dead during such event and the long-term propulsion should not be affected. During such conditions, WTs are either turned off or field weakening is used to develop a fault tolerant control (FTC) by the help of power electronics for the WT. FTC helps the machine not to be turned off completely, but less power is generated during fault conditions. An alternative efficient field weakening method using a Dual Rotor PMSM was suggested for both the applications. The DR-PMSM has two rotors instead of one, with identical surface mounted magnets on both rotors. One of these rotors has the capacity to rotate with respect to the other, in order to reduce the flux or completely short the flux path by misalignment of rotors [1]. The machine stator is exactly like the conventional PMSM. The machine is capable of reducing the induced emf to zero by field weakening.

In this thesis a transient 3D finite element model is presented to test the credibility of the machine. A 2D FEM of a conventional PMSM was also built to check the validity of the machine. It is seen that torque is a function of the active length of the machine, and if a gap is introduced between the rotors then the total length of the machine must be increased. Also, axial flux component which induces eddy currents in the stator teeth was studied. By modeling anisotropy in the stator iron, certain hot spots could be seen in the middle part of the stator. The forces that were in the shifting mechanism were studied and it was concluded that machine cogging can be reduced to reduce the effect of these forces. A machine prototype was also built which confirms the field weakening capability of the machine.

The DR-PMSM works like a conventional PMSM but with flux weakening capabilities and can be implemented on marine and wind turbine applications for these type of fault conditions.

Acknowledgements

I would like to begin by praising and paying my humble gratitude to the God Almighty. Blessings bestowed upon me by God Almighty are countless.

The research conducted in this MSc. thesis would not have been possible without the support and guidance of several individuals to whom I owe sincere gratitude and respect.

Firstly, I would like to extend my profound gratitude and appreciation to my daily supervisor Professor Robert Nilssen for providing me with the opportunity to work with Rolls Royce Marine AS on this thesis and for his continuous guidance through out the course of my thesis.

My deepest thanks to my co-supervisor Prof. Henk Polinder for being critical and helping me narrow down my research. I would also like to thank my co-supervisor Astrid Røkke for always helping me and getting me out of tough situations.

I really appreciate the help I got from Lars Ottar-Rolls Royce Marine, Hallvar Haugdal-NTNU and Faisal Wani-TU Delft with 3D modeling in COMSOL. There help has been invaluable to me.

I would also like to take this opportunity to express my deeply felt gratitude towards my parents and siblings for their selfless support and patience. Last but most certainly not the least, I sincerely appreciate all of my friends and colleagues for sticking with me through thick and thin, my apologies for not mentioning each one of them by their names. Any amount of thanks will be less than what they deserve.

Muhammad Usman Hassan
European Wind Energy Master

Table of Contents

Abstract **i**

Acknowledgements **iii**

Table of Contents **vii**

List of Tables **ix**

List of Figures **xii**

Abbreviations **xiii**

1 Introduction **1**
1.1 Background 1
1.2 Motivation 2
1.3 Problem statement 3
1.4 Research Question 3
1.5 Scope of the thesis 3
1.6 Outline of the thesis 3

2 Permanent Magnet Synchronous Machines (PMSM) **5**
2.1 Overview 5
2.2 Classification of PMSM 6
2.3 Permanent magnet materials 6
2.4 Rotor Configurations 7
2.5 Windings in electrical machines 7
2.6 Concentrated and distributed windings 9
2.7 Conclusion 10

3 Faults in PMSM **11**
3.1 Stator Faults 11
3.2 Direct driven permanent magnet synchronous generators(DD PMSG) for wind turbine 14
3.3 Electric propulsion generators for marine applications 15
3.3.1 DNVGL Requirements 16

4 Field Weakening in PMSM **17**
4.1 Introduction 17
4.2 Double Salient Permanent Magnet (DSPM) machine 18
4.3 Two part rotor synchronous PM machine 20
4.4 Flux barrier PM Machine 20
4.5 Consequent Pole Permanent Magnet (CPPM) machine 21
4.6 Brush-less PM Machine mechanical shaft rotor displacement . . . 22
4.7 Dual Rotor Permanent Magnet (DRPM) machine 23
4.8 Selected Machine 26

5 Electromagnetic Theory **29**
5.1 Maxwell Equations 29
5.2 Constitutive Relationship and Continuity 29
5.3 Magnetic Vector and Scalar Potential 31
5.4 Boundary conditions 32
5.5 Maxwell's Stress Tensor 32

6 Finite Element Modelling using COMSOL Multiphysics **35**
6.1 Finite Element Modelling 35
6.2 COMSOL Multiphysics 36
6.3 Machine Modelling in 3D 37
6.3.1 Assumptions 37
6.3.2 Geometry 37
6.3.3 Material Properties 38
6.3.4 Defining Physics 39
6.3.5 Setting up Mesh 40
6.3.6 Setting up solvers 41
6.3.7 Post-Processing 42
6.4 Results and Observations 42
6.4.1 Validity of the machine model 42
6.4.2 Voltages 44
6.4.3 Forces 46
6.4.4 Flux in the stator 49

7 Machine Prototype and Experiments **55**
7.1 Introduction 55
7.2 New prototype 55
7.3 Setup 57
7.4 Experiments 58
7.5 Results 59

8 Conclusions and Future Work **61**
8.1 Conclusion 61
8.2 Contributions 62
8.3 Future Work 62

Bibliography **65**

Appendix **71**

List of Tables

4.1 Machine Parameters 26

7.1 Machine Parameters for the DR-PMSM prototype 56

List of Figures

2.1 Rotor configurations 7
2.2 Double layer winding layout for 2 poles 18 slots PMSM[2] 8
2.3 Double layer winding by star slot method describing 2 poles 18 slots machine [2] 9
2.4 Distributed and concentrated windings 9

3.1 Stator winding short circuit [3] 12
3.2 Types of faults marked as 1, 2 and 3 [4] 13
3.3 Deltawinds Piet de Wit wind farm fire[5] 14
3.4 Directly driven on-shaft generator for marine propulsion 15

4.1 Double Salient Permanent Magnet (DSPM) machine with flux control [6] 18
4.2 DSPM with field weakening capabilities 19
4.3 Outer rotor DSPM with field weakening capabilities[7] 19
4.4 Construction of Two rotor synchronous PM machine [8] 20
4.5 Cross section of flux barrier PM machine [9] 20
4.6 Construction of Consequent Pole Permanent Magnet (CPPM) machine [10] 21
4.7 Magnetization and demagnetization of CPPM 22
4.8 Brush-less PM Machine mechanical shaft rotor displacement . . . 23
4.9 Dynamo electric machine[11] 24
4.10 Machine characteristics[11] 25
4.11 Construction of the dual rotor PMSM [1] 25
4.12 Winding layout for 10 pole 12 slot machine 27
4.13 Double layer winding by star slot method describing 10 pole 12 slot machine 27

4.14 Double layer winding conventional PMSM- 2D model 27

5.1 Typical ferromagnetic material magnetization characteristics[12] . 30

6.1 Steps for finite elemnet modelling in COMSOL 36
6.2 Machine geometry 38
6.3 Meshing of the machine 40
6.4 Meshing of stator 41
6.5 Induced emf and terminal voltage for DR-PMSM 43
6.6 Induced emf and terminal voltage for conventional PMSM 43
6.7 Mechanical and Electrical power of the PMSM 44
6.8 Induced emf and terminal voltage at 180 degrees 45
6.9 Phasor Diagram : Terminal voltage, induced emf and current for phase A 45
6.10 Voltage in phase A at various rotor positions 46
6.11 Rotor 1 is selected, top view of the PMSM 46
6.12 Axial forces on rotors and Torque at no load 47
6.13 Axial forces on rotors and Torque at loaded conditions 48
6.14 Axial torques on rotors 49
6.15 Airgap flux density of the machine on Rotor 1 50
6.16 Area of interest: middle region of stator 50
6.17 Axial magnetic flux density, ***Bz***, in the middle of the stator 51
6.18 Change in ***Bz*** as observed on a point A on stator teeth 52
6.19 Change in direction of current w.r.t. current density norm 53

7.1 The PMSM setup 56
7.2 Stator and the rotor of the dual rotor machine 57
7.3 Winding layout of 36 slot 18 pole for DR-PMSM 57
7.4 Connection diagram 57
7.5 Voltages on one coil while shifting of magnets from 0 degrees on wards 58
7.6 Voltages on one coil while shifting of magnets to 180 degrees . . . 58

8.1 Eddy currents in laminated core 71

Abbreviations

Symbol	=	definition
DD	=	Direct Drive
DR-PMSM	=	Dual Rotor Permanent Magnet Synchronous Machine
DSPM	=	Double Salient Permanent Magnet
DNVGL	=	Det Norske Veritas Germanischer Lloyd
FEM	=	Finite Element Modelling
FTC	=	Fault Tolerant Control
PMSG	=	Permanent Magnet Synchronous Generators
PMSM	=	Permanent Magnet Synchronous Machine
WT	=	Wind Turbine

Chapter 1

Introduction

1.1 Background

Large permanent magnet machines which are directly driven with low speed and high torque are mostly used as generators in wind turbines, motors for ship propulsion, or as actuators for thrusters or winch applications, at least in Norway [13]. The industries heavily rely on their efficient function of these machines. The two applications which are primarily focused in this thesis are permanent magnet machines for wind turbines and ship propulsion generators. For electric machines, about 30-40 % of the faults are related to stator insulation [14]. For offshore applications, the challenging operating environment makes the electric machines more vulnerable to failures. A survey focusing on electric motors used in offshore applications highlights that most faults are due to bearing or stator winding defects [15]. An insulation failure can cause a short circuit in the windings giving rise to fault currents which can demagnetize the rotor permanent magnets. An insulation failure can be catastrophic because it takes around 30 seconds to expand and could lead to destruction of stator core [16]. These failures affect the efficiency of machines and can be hazardous if not dealt on time; they can lead to a fire on marine vessels or on wind turbines.

Rolls Royce Marine AS is driven to make their products safer and reliable. They are also interested in a more reliable and efficient way to solve this problem for their PM shaft generators for ship propulsion. This thesis focuses on the way to control faults and avoid complete shut down of the propulsion system and wind turbine generators.

Research has shown that these types of faults develop gradually, which gives an opportunity to control the fault currents before they reach dangerous limits. Field weakening is a way to limit these fault currents by controlling the airgap flux in the machine. The idea is to make the induced currents practically nil by reducing the air-gap flux to zero. Field weakening in PM machines is a challenge, as the total inductance of the machine is large andX_d is small. Some researchers use low-coercive magnets and control the magnetization state of the magnets by injecting d-axis stator currents in the stator windings. In wind turbines permanent magnet synchronous generators (PMSGs), fault tolerant control (FTC) uses field weakening to control the airgap flux perceived by the stator windings by the use of power electronics. This is achieved by controlling the d-axis current in the windings, and for this, advance controlling techniques are required [17]. These methods have their limitations which do not give flexibility in flux weakening that these applications require. Many mechanical solutions to achieve flux weakening in PM machines have been proposed by inventors and researchers, which promise the needed flexibility to applications. In this thesis, the author looks for the best possible way to implement field weakening in these applications.

1.2 Motivation

After an extensive literature review of different patented radial flux permanent magnet machines with field weakening capabilities, dual rotor permanent magnet synchronous machine (DR-PMSM) was chosen. Both applications required a PMSM mounted on a shaft with surface mounted magnets on an inner rotor with flux weakening capabilities. This PMSM has two rotors instead of one, with identical surface mounted magnets on both rotors. One of these rotors has the capacity to rotate in order to reduce the flux or completely short the flux path by misalignment of rotors [1]. The machine stator is exactly like the conventional PMSM. The machine construction is explained in later chapters. As the construction of the DR-PMSM is different from conventional PMSM, so in order to gain understanding of the machine capability of flux weakening, best method should be adopted.

For studying all the complex effects in DR-PMSM such as eddy currents, non-linear characteristics of the machine, flux densities and other complex effects due to the complex geometry of the machine, FEM is the most accurate and feasible option rather than any analytical method.

A 2D FEM model can be implemented for conventional PMSM and machine performance can easily be studied. As DR-PMSM has characteristics of flux weakening, and during machine operation there are certain hot spots in stator due to eddy currents, which necessitated the need for 3D FEM.

The author has not found any previously done 3D FEM for DR-PMSM. Also, a laminated structure of iron inside the PMSM requires modeling of an-isotropic material which can only be modelled in 3D. These areas have not been researched and are of interest.

1.3 Problem statement

3D FEM of PMSM to accurately determine the induced voltages in windings under flux weakening operation. Simultaneously, magnetic forces and eddy currents due to the field weakening mechanism are to be investigated.

1.4 Research Question

To avoid complete shut down of wind turbine generators and shaft generators for marine applications, is flux weakening using DR-PMSM a valid solution?

1.5 Scope of the thesis

1. Investigate current ways for field weakening applications for PM machines.

2. Develop and describe a 3D transient model for the dual rotor PMSM

3. To estimate the magnitude of the axial component of magnetic flux density, and its impact on the electromagnetic forces developed in the machine.

4. Develop a DR-PMSM prototype to test and verify the flux weakening capability of the machine.

1.6 Outline of the thesis

1. **Chapter 2** Explains the important design parameters for PMSM which are important for the discussed applications and machine design

2. **Chapter 3** Explains the types of faults in PMSM that are the focus of this thesis and how they are dangerous for wind turbines and marine applications.

3. **Chapter 4** Explains the use of field weakening in PMSM as a fault mitigation technique. It also highlights various radial flux PM machines researched, in search of for a mechanical solution for stator faults.

4. **Chapter 5** Explains basics of electromagnetic theory necessary for understanding FEM

5. **Chapter 6** Explains how to implement FEM for modeling a 3D PMSM using COMSOL multiphysics. Also, results of the simulations are discussed.

6. **Chapter 7** Describes the machine experimental setup for testing the simulations. The results from the experiments comments on the practicality of the machine.

7. **Chapter 8** Concludes the thesis and highlights what can be done in future regarding this topic.

Chapter 2

Permanent Magnet Synchronous Machines (PMSM)

Chapter Summary: This chapter starts with an overview of Permanent Magnet Synchronous Machines. The basic design construction parameters which are of interest are presented.

2.1 Overview

Permanent magnet synchronous machines (PMSM) are excited by a permanent magnet and not by a coil. A synchronous machine rotates with a fixed frequency constantly at synchronous speed in the steady state.

These machines are generally used commercially for conversion of mechanical to electrical energy and directly connected to a power grid. Due to commercial production of high end permanent magnetic materials several industries have shifted to the use of PMSM and with the passage of time, industries where electric machines are being used, often prefer PMSM.

The basic construction of PMSM consists of a rotating rotor in the center which has magnets and a stationary stator constituting of windings. In generator mode, torque is given to the rotor causing a rotation and a subsequent changing magnetic field which flows through the conductors. The resulting induced voltage in the conductors then converts mechanical energy into electrical energy.

The rotor magnetic field is established by permanent magnets and they are normally arranged in order to generate maximum field or arranged differently for field weakening. Usually, the coils are placed in various winding layouts in order to generate high voltages. These voltages are called induced voltages. The frequency (f) of the induced voltage and speed of the rotor are related as

$$n = \frac{120f}{p} \tag{2.1}$$

n is the rotor speed in rpm and p is the number of poles

2.2 Classification of PMSM

The PMSM come in many shapes and sizes. The machine geometry depends a lot on the application. Following are some of the classification of PM machines;

- Inner or outer rotor
- Slotted or slotless stator
- Surface mounted or interior rotor magnets
- Axial or radial flux
- Distributed or concentrated windings.

2.3 Permanent magnet materials

Permanent magnets can be as desired and magnetized in a direction of choice. They normally consist of bonded or sintered materials. The quality of materials is continuously improving and PMs are becoming more insensitive to external fields. The only major risk of demagnetization is from short circuits in hot machines as in the application researched in the thesis.

PM materials commonly used commercially today are:

- **Ferrite Magnets:** They are low cost with high electric resistivity and have linear behaviour. The have low B_r
- **AlNiCo magnets:** They have low temperature coefficients, very low coercivity and have non linear behavior
- **Rare Earth Cobalt (RECo) magnets:** They have a higher cost, high magnetic properties and have linear behaviour.
- **Neodymium (NdFeB) magnets:** They have the highest magnetic properties, high temperature co-efficient and are linear.

2.4 Rotor Configurations

There are different ways a rotor can be configured by placing magnets in a certain way. As shown in figure 2.1.

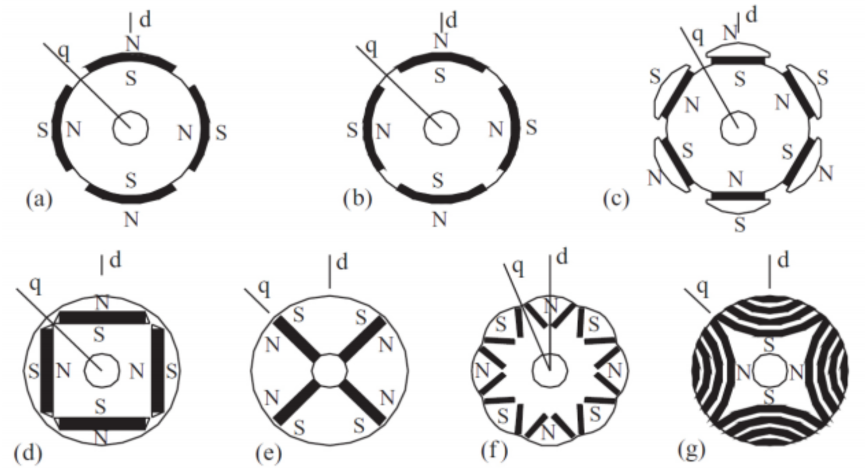

Figure 2.1: Rotor configurations: (a) surface mounted (b) Surface mounted inset (c) surface magnets and pole shows (d) tangential (e) spoke (f) V type rotor (g) PM assisted synchronous reluctance motor [18]

Surface mounted permanent magnets (SPM) are most commonly used magnets in PMSGs. They are usually radially magnetized. As the magnets can be attached to the surface makes the construction simpler and cheap [18].

2.5 Windings in electrical machines

When every slot has one coil side it is known as *single layer* winding and when every slot contains two coil side each they are known as *double layer* winding. When they contain three or more coil side then they are known as *multilayer* winding.

Single layer windings have higher slot utilization because of elimination of inter-layer insulation. Single layer windings have better distribution factor but they have high levels of sub-harmonics giving rise to high rotor losses. While double layer windings help reduction of cogging torque and sub-harmonics.

Windings are either referred to as *integer* or *fractional slot windings* depending if the factor **q** is an integer or a fractional number. Where q is basically a number of slots per pole per phase, it is expressed as:

$$q = \frac{Q}{mp} \tag{2.2}$$

where Q is the number of slots, p is the number of poles and m is the number of phases

The winding layout is defined on the slot relative electrical position. Every slot is separated by angular slot pitch, γ_s and it is given in electrical degrees.

$$\gamma_s = \frac{\pi \cdot p}{Q} = \frac{\pi}{q \cdot m} \tag{2.3}$$

Depending upon the phase spread,σ_e, every slot is assigned a phase and it is usually $\frac{\pi}{3}$ rad. [2].

For a symmeteric 3-phase layout, two conditions are defined for single and double layer winding respectively.[19]

$$\frac{Q}{6} \in \mathbf{N} \qquad\qquad \frac{Q}{3} \in \mathbf{N} \tag{2.4}$$

where **N** is set of all natural numbers.

Professor Robert Nilssen has developed an application for laying out single and double layer windings for concentrated coils based on star slot method explained in [20] and [19] laying out concentrated windings for machines. The software automatically gives the winding layout by distributing the phases to achieve maximum harmonic magnetomotive force (MMF). An example of double layer winding is given in the table below, where p is 2, Q is 18 and m is 3.

Slot #	1	2	3	4	5	6	7	8	9	10	11	12	13	14	15	16	17	18
Phase R	R	R	R							-R	-R	-R						
Phase S							S	S	S							-S	-S	-S
Phase T				-T	-T	-T							T	T	T			
RST	R	R	R	-T	-T	-T	S	S	S	-R	-R	-R	T	T	T	-S	-S	-S
Bottom	R	R	R	-T	-T	-T	S	S	S	-R	-R	-R	T	T	T	-S	-S	-S
SingleP																		

Figure 2.2: Double layer winding layout for 2 poles 18 slots PMSM[2]

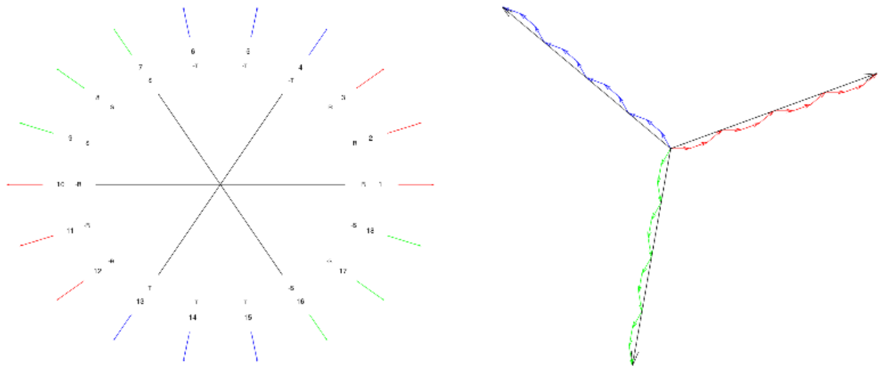

Figure 2.3: Double layer winding by star slot method describing 2 poles 18 slots machine [2]

2.6 Concentrated and distributed windings

The coils that have non-overlapping end windings are called concentrated windings. The $q < 1/2$ for concentrated windings

The coils that have overlapping end windings are called distributed windings. Usually, several coils are distributed over one pole in this type of windings. The $q > 1/2$ for distributed windings.

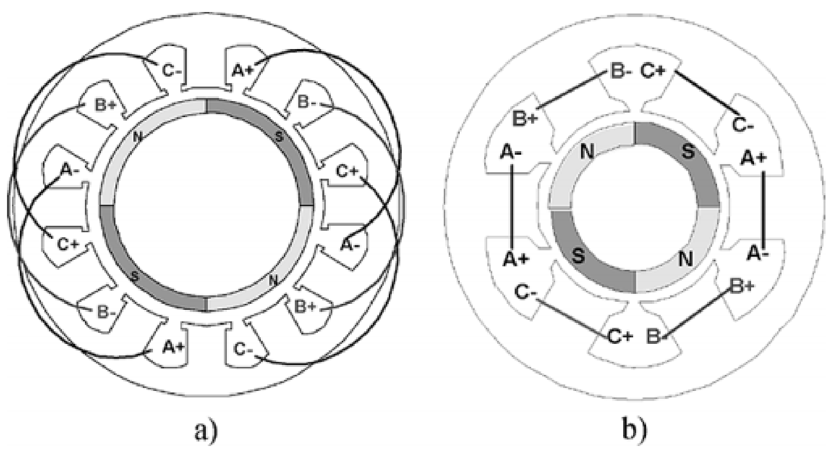

Figure 2.4: (a) Distributed winding (b) Concentrated winding [21]

Distributed windings are preferably used with machines which have bigger poles and a large number of slots per pole. With these windings higher order harmonics can be eliminated. The concentrated windings have less cogging and with fractional slot windings certain harmonics can be eliminated. Concentrated windings have compact end windings and have simpler construction [22]. There are merits and demerits of both concentrated windings and distributed windings. So the choice of a winding depends upon the machine design priority.

2.7 Conclusion

The PMSMs applications under discussion are DD PMSG for wind turbines and shaft generators for marine propulsion drive train. Both of these applications have an inner rotor structure because it offers better stability as the whole rotor is directly attached to the shaft. The rotor will have surface mounted NdFeB magnets which are radially magnetized. This offer simple assembly and NdFeB magnets are the most common magnets due to their high energy product and magnetic remanence. The stator will have concentrated windings as both machines require less cogging and it has a simpler construction of the windings.

Chapter 3

Faults in PMSM

Chapter Summary: As faults related to stator windings and insulation degradation are the focus of this thesis. Therefore, this chapter explains what are stator faults and how they are dangerous for PMSM applications.

3.1 Stator Faults

The faults which occur in the stator of the alternator are called stator faults. Stator faults are caused by the breakdown of insulation due to high temperature rising of the overload conditions and the high voltage stress. The simplest form of stator fault is shown in figure 3.1 which shows the i_f, circulating currents due to short circuits, are against the phase currents i_s currents. These currents induce magnetic fields which are opposite to the flux of the machine [23]. If the fault is not detected timely then this fault can become worse and can cause demagnetization faults in rotor permanent magnets [3].

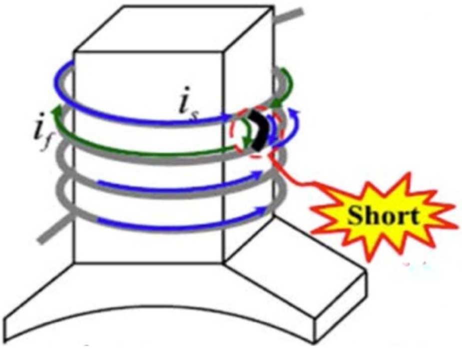

Figure 3.1: Stator winding short circuit [3]

Permanent Magnets are the most crucial components of PMSM, as they produce torque by generating fluxes in the air-gap. They under go a change in their characteristics by temperature variation or by induced magnetic fields which oppose the PM magnetic field. They can partially or completely lose their characteristics due to these faults. Irreversible demagnetization is basically the loss of magnetization when PM demagnetization curve does not return to its original state.

Both of these faults, winding turn faults and demagnetization fault of PM are correlated to each other. It means that one fault can bring out the other one. Short-circuit faults in the stator are particularly hazardous in permanent magnet machines, as these faults produce magnetic field intensity higher than the coercivity of the magnets, demagnetizing the machine magnets and damaging the machine.

The three types of inter turn faults which are focus of this study.

1: turn-to-turn short circuit in one strand;

2: turn-to-turn between parallel strands;

3: turn-to-turn short circuit between two phases.

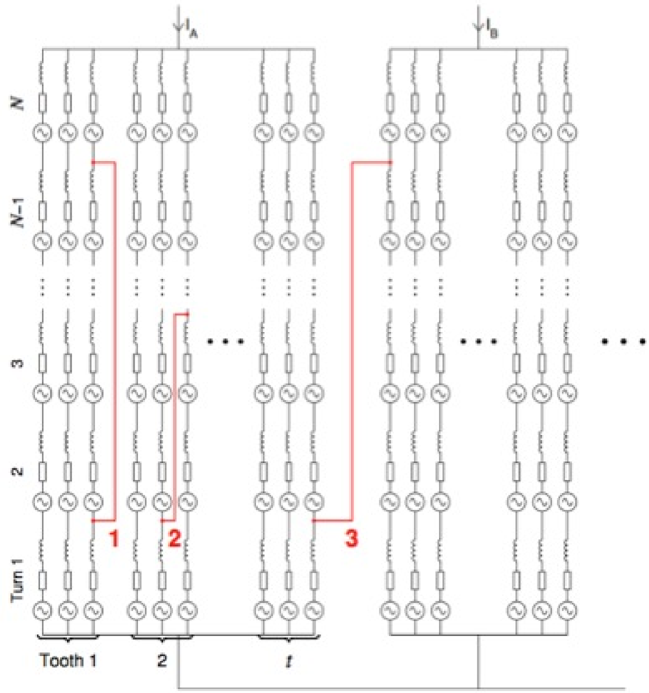

Figure 3.2: Types of faults marked as 1, 2 and 3 [4]

Geest talks about these faults in details in his Ph.D. thesis [4] and how they affect the performance of PMSMs. A single strand short circuit, as marked with 1 in figure 3.2, is the most severe faults in inter-turn faults and they most likely occur adjacent to each other in a slot. As the turn resistance limits the fault currents with in fewer turns involved, the losses depend on the square of the frequency.

These losses are large because the healthy and shorted parts of the affected strand behave as an auto-transformer. Therefore, only a few turns of healthy coils can induce several tens of amperes in the shorted ones.

Turn-to-turn short circuit between parallel strands, as marked with 2 in figure 3.2, is the less severe fault and turn to turn short circuit in the neighbouring teeth/phases lies between the other two in terms of severity. Turn-to-turn faults are resistance dependent in very high speed machines. This means that turn-to-turn faults are more severe in high speed machines than line frequency machines.

Usually an internal fault in the generator produces second harmonic currents which can be easily detected by differential protection schemes. The mitigation time is usually 0.2-0.5s in which the fault should be neutralized [23].

3.2 Direct driven permanent magnet synchronous generators(DD PMSG) for wind turbine

In recent years there has been increased demand for permanent magnet synchronous generators, which are directly driven, due to their low maintenance as compared to geared ones [2]. Due to increased size of the modern DD PMSG, many problems have arisen.
At Risø National Laboratory, Denmark, a survey on generators and power electronics have been carried out in 2001[24]. The comments suggest that PMSM have some uncertainties regarding maintenance due to high temperatures. These faults in PMSM occur in high number in bearings and stator windings[25]. The internal winding faults can raise the temperatures of the windings and may raise certain hot spots in the machine. As explained before, generator electro-mechanical faults are the focus of this thesis, which are the most common wind turbine faults besides gearbox and power converter faults [17].For electric machines, about 30-40 % of the faults are related to stator insulation [14].

As explained earlier, these failures can be catastrophic and can result in completely damaging the stator core. These faults gradually develop and can be controlled if preventive actions are taken. In [17] Vinko and Mario explain a fault tolerant control (FTC) for DD-PMSG, which uses field weakening, to reduce fault currents by changing the airgap flux density. This enables the PMSG to operate during faults and prevents complete shut down of the generator. This thesis searches for another method of field weakening to cater this problem. The figure 3.3 shows a catastrophic failure of wind turbine due to short circuiting and resulting in the death of two service engineers in 2013[5]. The incident occurred during maintenance, which demands the implementation of more efficient and better fault mitigation techniques.

Figure 3.3: Deltawinds Piet de Wit wind farm fire[5]

3.3 Electric propulsion generators for marine applications

The idea of using electric power for ship propulsion system is not new and has been used since the beginning of the twentieth century [16]. As the ship is fully electric their vital systems like navigation etc. depend upon electric power. To design the propulsion and integrated power a completely robust one, there should be fault tolerant and no interruption of power is necessary. Moreover, it should be able to operate in case of failure by re-configuring itself. Therefore, timely electric propulsion machine diagnosis is crucial for continuing a trouble free operation of electric ships. For propulsion, electric ships use induction motors, synchronous motors or PM synchronous motors. Electric machines and drives have very low maintenance requirement but ship's environment can make it more prone to failures. Thus, timely detection and mitigation of faults are required before things lead to catastrophic events.

The research work focus will be mitigation of faults by controlling the flux in PM machines. This problem is relevant for all applications of large PMSM which are directly driven. The research problem is currently center of discussion in Rolls Royce Marine AS.

The application to be researched is an on-shaft PMSM which is a part of hybrid propulsion drive train for marine vessels, as shown in figure 3.4. As earlier mentioned, the short circuit faults in the stator windings can be catastrophic which can result in a fire on board. To ensure the safety on board, the shaft generator should be up to the mark of IMO (international maritime organization) rules and regulation, DNVGL ensures and certifies all the marine shipping equipment.

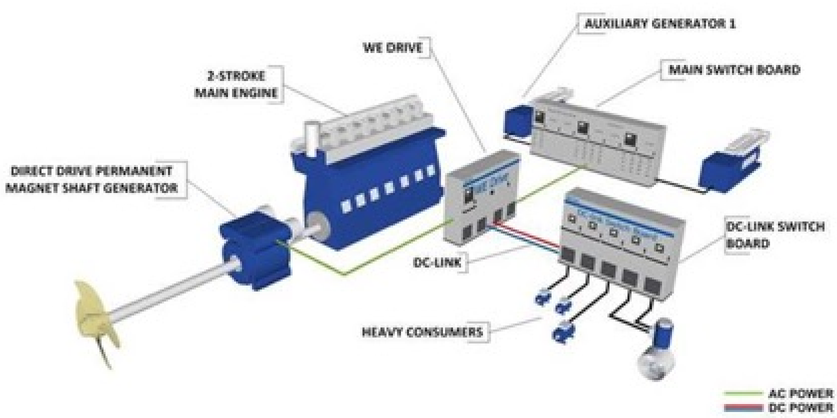

Figure 3.4: Directly driven on-shaft generator for marine propulsion

3.3.1 DNVGL Requirements

The requirements state that all operating modes should be designed that in a case of a fault in the control system the propulsion is not disabled permanently.

For this there are three types of redundancies that were described in DNVGL rules and regulations for equipment in electrical ships [26], that should be followed.

1. R1 type redundancy ensures that if there is a fault within the electric system or control system, the power of maneuverability should be restored with in 30-45 seconds after mitigating the fault or after the loss of power.
2. In case of internal failure, the PM machine should be made electrically dead(there should be no flow of power). For this R2 type redundancy is valid for internal failures which are; for 10 minutes the propulsion can be deactivated to mitigate the fault or to deactivate the machine.
3. R3 type redundancy in case fault mitigation requires more time and machine requires repairs. In this, propulsion can be stopped for 3 hrs and the shaft can be at a stand still during the repair procedure.

To ensure safety on board, these requirements must be met by Rolls Royce Marine AS for the use of PM machines for this application. If the PM machine complies with R2 redundancy requirements than R3 redundancy is not necessary. This thesis checks for suitable solutions for marine applications, which meet the DNVGL, R2 and R3 type redundancy, requirements.

Chapter 4

Field Weakening in PMSM

Chapter Summary: This chapter explains all the types of radial flux PMSM capable with field weakening and why one particular PMSM have been chosen for our applications.

4.1 Introduction

After discussions with the team at Rolls Royce and DNVGL, it was finalized that a field weakening method can be adopted to fulfill the DNVGL requirements. In this thesis, the work is focused on this marine application and the research looks into possibilities of a common solution for wind turbine applications.

Field weakening is simply manipulating the airgap flux of the machine, in order to control the induced voltages in the machine. It is rather simpler to implement field weakening in field wound machines as the airgap flux can just be controlled by the changing the excitation current. In PM macines the magnetic field intensity of PM is fixed and this makes it a challenge to control the airgap flux. In order to implement field weakening in PM machines either it is done by control techniques or by enhancing the machine topology. For manipulating air gap flux using control techniques, stator d-axis current is controlled to manipulate the flux in the stator or controlling the magnetization states of low coercive magnets. Vinko explains FTC for PM wind turbine generators [17] but the limitation of his method is unsymmetrical stator currents. R. D. Lorenz explains the technique for active control of d-axis current for variable flux PM machines in his research [27] using low coercive magnets. There is higher risk of demagnetization using control techniques as they can cause serious demagnetization of magnets and high losses [28]. Both the techniques discussed have their limitations and therefore they are not further researched in this thesis. Another way to implement field weakening is by changing machine topology. The PM machine designers have come up with brilliant ways to develop radial airgap flux machines capable of field weakening. Following are some of the PMSMs capable of field weakening researched for this thesis.

4.2 Double Salient Permanent Magnet (DSPM) machine

The Double Salient Permanent Magnet (DSPM) machine uses high energy magnets into its doubly salient structure of the synchronous reluctance machine. The magnets can either be placed in the rotor or the stator. [29] [30]. In this particular design, the machine stator has high energy NdFeB magnets and these magnets can be shorted by changing the reluctance path of the PM machine. This is done by rotating the magnetic collar by 30 degrees. The flux will be completely shorted in case the magnetic part of the collar faces the stator magnets. This can be observed in figure 4.1b. The rotor construction of DSPM machine resembles that of variable reluctance machine composed of laminated sheets.

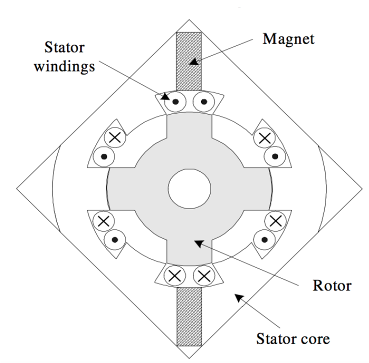

(a) Cross-section of DSPM

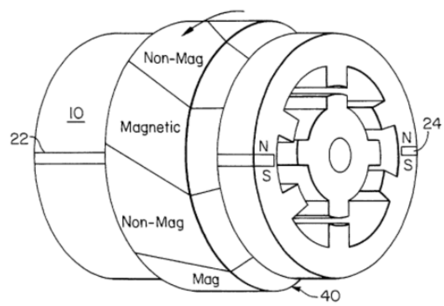

(b) Machine construction

Figure 4.1: Double Salient Permanent Magnet (DSPM) machine with flux control [6]

These machines are good for electric vehicles and most adjustable speed drive applications.

Another variation of DSPM is shown in figure 4.2. The ferrite magnets are lined in the circumference of the stator and a circumferential DC field winding is placed in the core. Both, the winding and the magnets, produce the magnetic flux in the same trajectory. The flux can be weakened or boosted by changing the direction of the current. High flux density can be achieved with large magnet surface area.

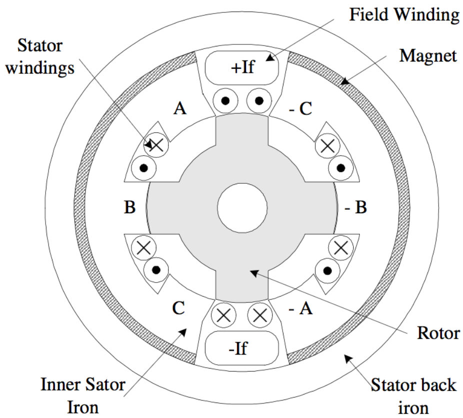

Figure 4.2: DSPM with field weakening capabilities

Another type of DSPM is shown in figure 4.3. The machine has an outer rotor and magnets are embedded in the stator. This geometry of the machine increases the airgap diameter which helps in reaching higher torques. This type of machine is already being used in the auto-mative industry.

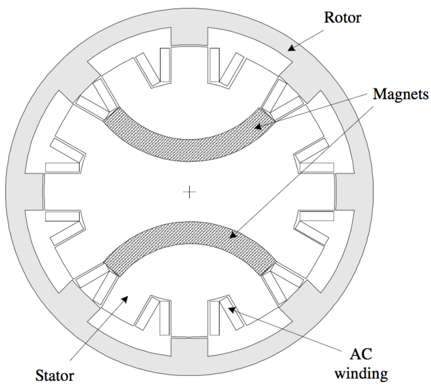

Figure 4.3: Outer rotor DSPM with field weakening capabilities[7]

To eradicate the flux completely in this machine is a challenge and also for large scaled PM machines this would be harder to implement.

4.3 Two part rotor synchronous PM machine

Another field weakening topology consists of two part rotor, one having a PM motor and the other a reluctance motor mounted together on a single shaft. The PM part has surface mounted magnets and reluctance section is axially laminated. The idea of this design is to have these two rotor sections modified to have the desired ratio of L_d/L_q [31]. These machines can be designed to have a fixed range of variable speed and are suitable for electrical vehicles.

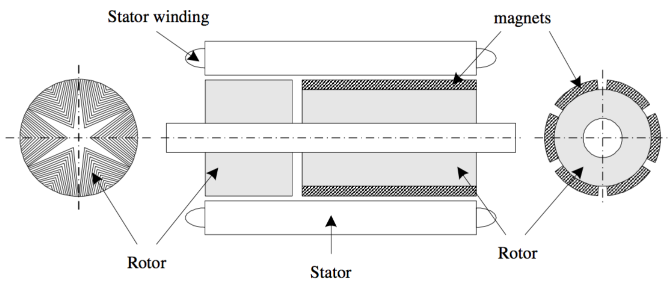

Figure 4.4: Construction of Two rotor synchronous PM machine [8]

4.4 Flux barrier PM Machine

Another variety of radial flux machine PM machine with flux weakening is shown in figure 4.5 [9]. This PM machine has iron mounted on the surface of the magnets. In between magnets, there are flux barriers. In total there are four iron sections and eight flux barriers. In this machine, I_d is used to modify the flux path instead of weakening the magnet flux. This way the magnet flux in the windings is decreased but the magnetic flux in the magnets is preserved. So demagnetization of magnets is no more a problem in this PM machine.

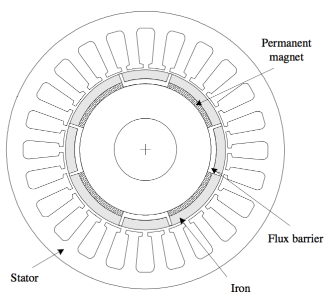

Figure 4.5: Cross section of flux barrier PM machine [9]

4.5 Consequent Pole Permanent Magnet (CPPM) machine

Consequent Pole Permanent Magnet (CPPM) machine is a comparatively simpler method for air gap flux control[10]. The machine stator is composed of a laminated core, solid iron yoke and 3 phase conventional winding with a circumferential DC winding placed in the middle of stator. The rotor poles are divided into two sections, one has radially magnetized surface mounted magnets and the other is a laminate iron pole. Figure 4.6 shows the construction of the machine.

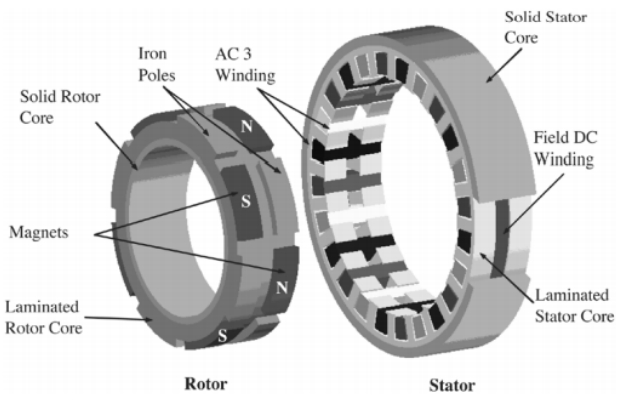

Figure 4.6: Construction of Consequent Pole Permanent Magnet (CPPM) machine [10]

The direction of the current in the DC winding determines the direction of air gap flux. The figure 4.7 clearly shows the air gap flux control phenomenon.

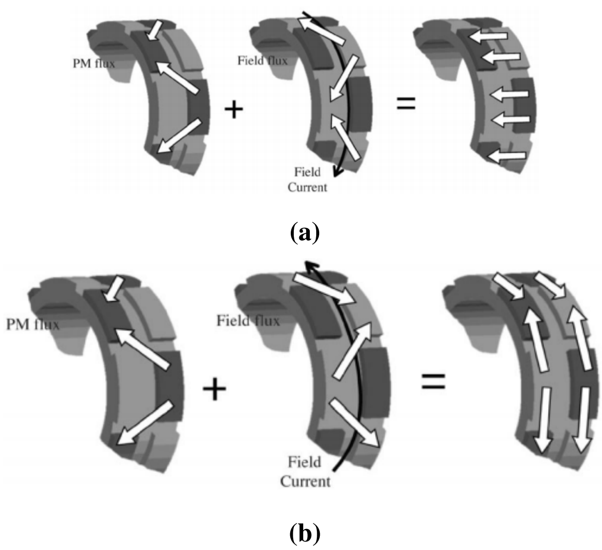

Figure 4.7: (a) Demagnetization of CPPM, flux moving axially. (b) Magnetization of CPPM

This machine has no demagnetization risk of PMs because of the rotor iron poles. Also, the ampere turn requirement for field winding is concluded to be lower. The machine can be used for a wide variety of applications but there are other disadvantages. One is the machine power density is lower because of the extra DC winding. There are also extra losses due to 3D flux distribution in the machine.

4.6 Brush-less PM Machine mechanical shaft rotor displacement

Another method for field weakening uses mechanical technique discussed in [32]. The brushless PM machine is operated from high to normal speed by reducing average flux per pole but the radial air gap is kept constant. This machine topology changes the axial misalignment of the PM rotor to weaken the field. By increasing the axial misalignment between rotor poles and stator reduces the effective flux going through stator as shown in figure 4.8.

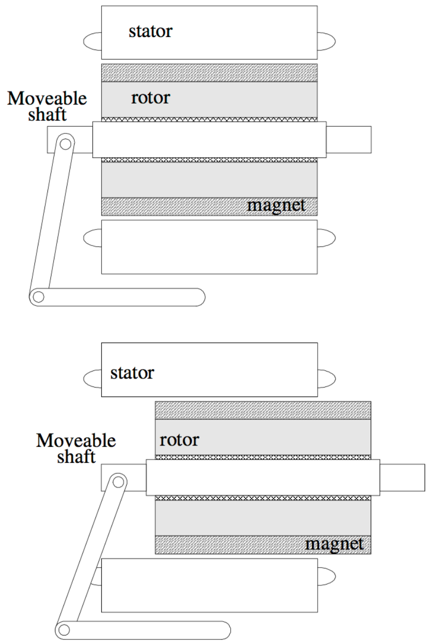

Figure 4.8: Brush-less PM Machine mechanical shaft rotor displacement

4.7 Dual Rotor Permanent Magnet (DRPM) machine

Dual Rotor Permanent Magnet (DRPM) machine is a novel PM machine with field weakening capabilities. The rotor is divided into two sections, the first section has own sets of alternating poles and the second section also has identical sets of alternating poles as shown in figure 4.9. One of these rotors has the capacity to rotate in order to reduce the flux or completely short it by misalignment of rotors. The idea of dual rotor arrangement can be applied to any surface magnet or interior magnet rotor structures.

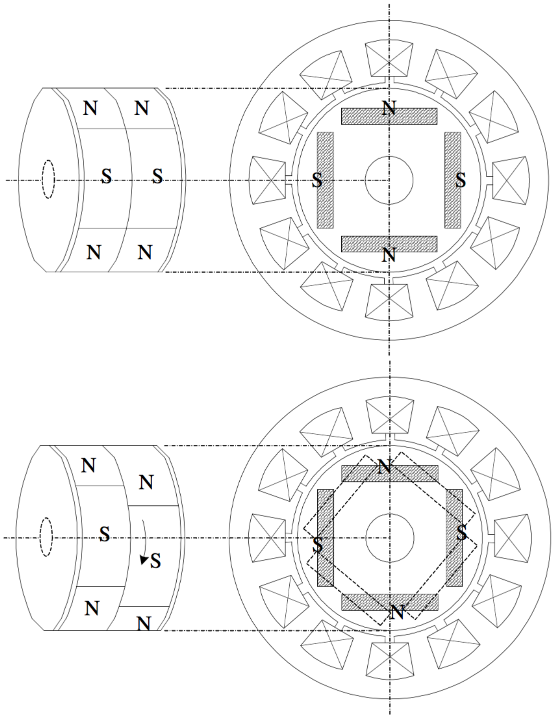

Figure 4.9: Dynamo electric machine[11]

This idea was first introduced by *Hitachi Ltd.* in the year 1998 [33]. Later it was modified by the company for electric vehicles and wind power generation systems in 2002 [34, 35, 11] and 2003 [36]. By misalignment of the two rotors, as shown in figure 4.9, the flux in the machine can be reduced and induced emf can be controlled along with terminal voltage. The figure 4.10 shows how by field weakening machine induced voltage and terminal voltage can be kept constant even at high speeds for traction applications.

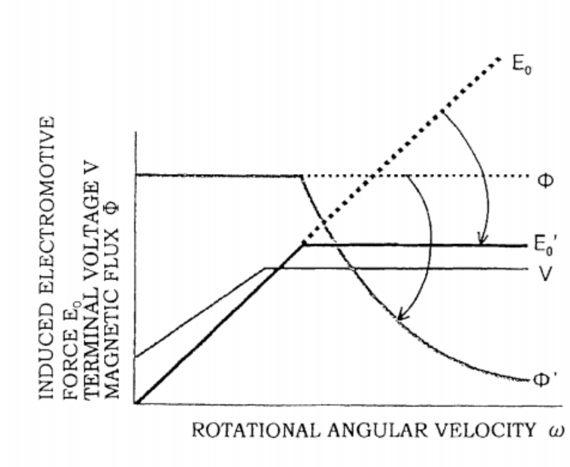

Figure 4.10: Machine characteristics[11]

In the year 2009, R. D. Bremner devised a simple gear mechanism for the shifting of magnets or misalignment of rotors. The synchronous machine had a fixed gap between rotors and surface mounted magnets were used in the machine. The invention aims to have better field weakening by misalignment of the rotors while they are running [1]. The figure 4.11 shows the construction of the machine. Bremner's machine promises that back emf can be reduced to zero when the rotors

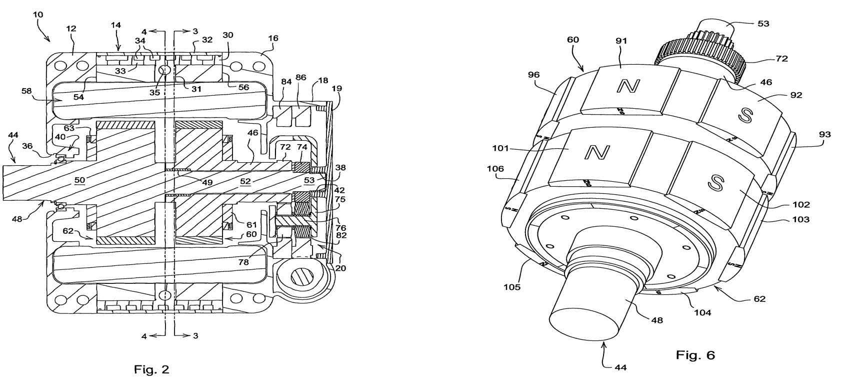

(a) Cross-section of the PMSM **(b)** Rotor Construction

Figure 4.11: Construction of the dual rotor PMSM [1]

are misaligned and flux is shorted.

4.8 Selected Machine

After reviewing various radial flux PMSMs and their ability to implement field weakening effectively, Bremner's machine design for DR-PMSM was shortlisted. It is the only PMSM which has the ability to completely reduce the back emf to zero once the magnetic flux path is shorted. Also, the idea of dual rotor arrangement can easily be implemented in the marine and wind turbine applications who have surface magnet or interior magnet rotor structures.

The thesis will look into how to implement a working 3D FEM model of the machine in COMSOL Multiphysics.

Machine used: The machine parameters were provided by Rolls Royce Marine AS to fit to there application. To make the modelling simplistic, 12 slot - 10 pole machine was chosen. The machine parameters used in the thesis are shown below.

Table 4.1: Machine Parameters

Parameter	**Unit**	**Value**
Machine Diameter	mm	800
Machine active length	mm	1000
Machine length	mm	1100
Rotor radius	mm	306
Airgap length	mm	10
Rotational Speed	rpm	115
Rated power	kW	410
Rated current	A	250
Poles	-	10
Stator slots	-	12
Winding layout	-	Double layer
Magnet length	mm	22
Remanent flux density	T	1.4

Here $q = \frac{2}{5}$, which implies that concentrated winding should be used as explained in section 2.5.

Slot #	1	2	3	4	5	6	7	8	9	10	11	12
Phase R	R					R	-R					-R
Phase S		S	-S					-S	S			
Phase T				-T	T					T	-T	
RST	R	S	-S	-T	T	R	-R	-S	S	T	-T	-R
Bottom	R	-R	-S	S	T	-T	-R	R	S	-S	-T	T
SingleP												

Figure 4.12: Winding layout for 10 pole 12 slot machine

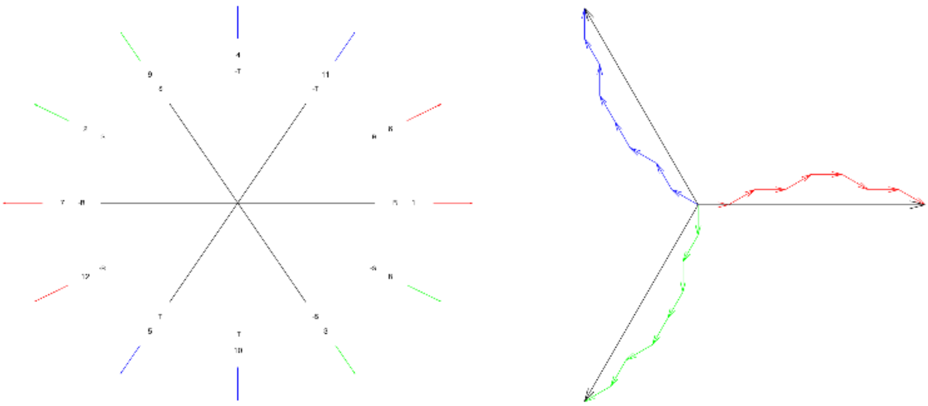

Figure 4.13: Double layer winding by star slot method describing 10 pole 12 slot machine

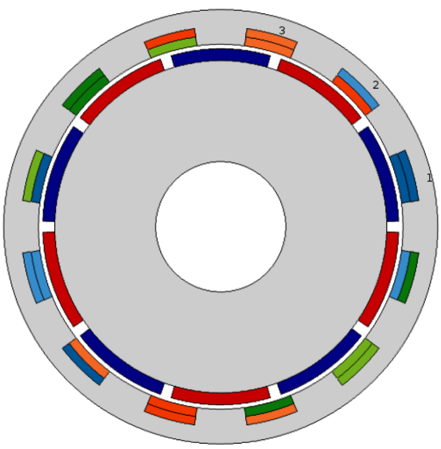

Figure 4.14: Double layer winding conventional PMSM- 2D model

Chapter 5

Electromagnetic Theory

Chapter Summary: This chapter explains basic of electromagnetic theory and the governing differential equation which is used in finite element modeling.

5.1 Maxwell Equations

In modeling electrical machines Maxwell equations are the backbone for describing all electromagnetic phenomenon. The equations presented below together with Lorentz force and equations of motion describe all electromagnetic conversions of interest in rotating machinery[37].

$$\bigtriangledown \times \vec{H} = \vec{J} + \frac{\partial \vec{D}}{\partial t} \tag{5.1}$$

$$\bigtriangledown \cdot \vec{D} = \rho \tag{5.2}$$

$$\bigtriangledown \times \vec{E} = -\frac{\partial \vec{B}}{\partial t} \tag{5.3}$$

$$\bigtriangledown \cdot \vec{B} = 0 \tag{5.4}$$

5.2 Constitutive Relationship and Continuity

Constitutive relationships are

$$\vec{D} = \epsilon_o \epsilon_r \vec{E} = \epsilon \vec{E} \tag{5.5}$$

$$\vec{B} = \mu_o \mu_r \vec{H} = \mu \vec{H} \tag{5.6}$$

$$\vec{J} = \sigma \vec{E} \tag{5.7}$$

The equation of continuity is

$$\bigtriangledown \cdot \vec{J} = -\frac{\partial \vec{\rho}}{\partial t} \tag{5.8}$$

The above relationships describe macroscopic properties of the medium being dealt with in terms of permeability μ, permittivity ϵ and conductivity σ. These quantities are not merely constants because theses relationships are generally non-linear. A notable phenomenon in the iron part of the machine is saturation. Saturation happens when magnetic flux density in the material can not increase further by increasing the applied magnetic field. **B-H** curves of various materials are shown below in figure 5.1.

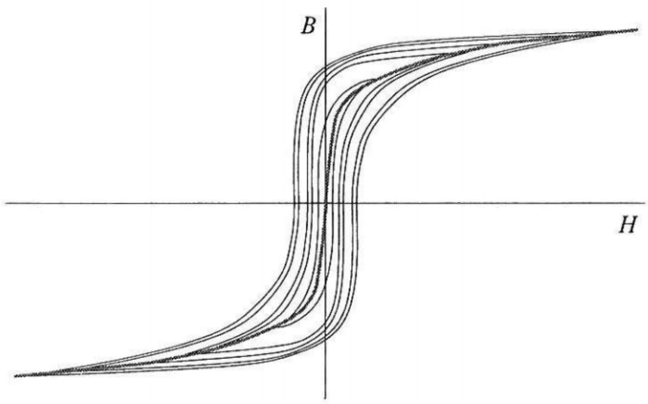

Figure 5.1: Typical ferromagnetic material magnetization characteristics[12]

In the thesis work, all the materials are considered linear, so the variation in the values **B-H** curve is not considered.

Generally, the media is non-isotropic, then these parameters depending upon material are treated as tensor quantity.[38]

$$\mu = \begin{bmatrix} \mu_x & 0 & 0 \\ 0 & \mu_y & 0 \\ 0 & 0 & \mu_z \end{bmatrix} \epsilon = \begin{bmatrix} \epsilon_x & 0 & 0 \\ 0 & \epsilon_y & 0 \\ 0 & 0 & \epsilon_z \end{bmatrix} \sigma = \begin{bmatrix} \sigma_x & 0 & 0 \\ 0 & \sigma_y & 0 \\ 0 & 0 & \sigma_z \end{bmatrix}$$

Mainly μ_i, σ_i and ϵ_i along the ith direction are not constant. They are a function of magnetic field $\vec{B}$ and electric field $\vec{E}$ or position.

5.3 Magnetic Vector and Scalar Potential

Magnetic field that possesses curl due to current density $\vec{J}$ is defined by Magnetic Vector potential A. Magnetic flux density $\vec{B}$ can be written as the curl of Vector field $\vec{A}$ [1].

$$\vec{B} = \bigtriangledown \times \vec{A} \tag{5.9}$$

The divergence of $\vec{A}$ can be defined in any way as fit for the problem situation. This choice of $\bigtriangledown \cdot \vec{A}$ is called **gauge fixing of A**. Most commonly for stationary or quasi-stationary magnetic fields *Coloumb's position* is used.

$$\bigtriangledown \cdot \vec{A} = 0 \tag{5.10}$$

For time variable electromagnetic fields *Lorentz's position* is used

$$\bigtriangledown \cdot \vec{A} = -\mu\epsilon \frac{\partial \vec{V}}{\partial t} \tag{5.11}$$

In stationary or quasi-stationary magnetic fields current displacement is neglected so from equations 5.1 and 5.9 we have:

$$\bigtriangledown \times \left(\frac{1}{\mu} \bigtriangledown \times \vec{A} \right) = \vec{J} \tag{5.12}$$

In case the permeability μ is constant, the materials are homogeneous and by using Coloumb's position then above is reduced to Poisson Equation. Mathematically it is given as:

$$\bigtriangledown^2 \vec{A} = -\mu \vec{J} \tag{5.13}$$

The above equation becomes the Laplace equation when the current density $\vec{J}$ is null in the problem.

$$\bigtriangledown^2 \vec{A} = 0 \tag{5.14}$$

If the gauge of A is not specified then it is not possible to have a solution for the potential and there is a larger chance of going into numerical instabilities in 3D modeling.

In case of zero current density, the equation 5.1 becomes,

$$\bigtriangledown \times \vec{H} = 0 \tag{5.15}$$

And hence magnetic field intensity $\vec{H}$ can be written as gradient of the scalar potential $\vec{\phi}$

$$H = - \bigtriangledown \phi \tag{5.16}$$

[1] Wani in his thesis [39], explains 3D magnetostatic modeling for induction machines using FEM. To understand various concepts, Wanis thesis was used for 3D FEM modelling of dual rotor PMSM.

In case $\vec{J}$ is not known, then from the equations 5.3 and 5.9:

$$\bigtriangledown \times \vec{E} = -\frac{\partial}{\partial t} \bigtriangledown \times \vec{A};\ \bigtriangledown \times (E + \frac{\partial \vec{A}}{\partial t}) = 0 \tag{5.17}$$

$$-\bigtriangledown V = E + \frac{\partial \vec{A}}{\partial t} \tag{5.18}$$

$$\vec{J} = \sigma(-\bigtriangledown V - \frac{\partial \vec{A}}{\partial t}) \tag{5.19}$$

If this is introduced to the equation 5.13:

$$\bigtriangledown^2 \vec{A} = -\mu\sigma(-\bigtriangledown V - \frac{\partial \vec{A}}{\partial t}) \tag{5.20}$$

5.4 Boundary conditions

The two boundary conditions need to be specified for ϕ are Dirichlet conditions and Neumann conditions. When the initial value is specified for the problem at a point and is part of the given geometry it is called **Dirichlet condition**, so in this case, initial value ϕ_0 should be specified. For homogeneous Dirichlet condition, it should be specified along with a line (at the boundary) which makes it equipotential. Neumann condition is basically when a normal derivative of potential is specified. Homogeneous **Neumann condition** is $\frac{\partial \phi}{\partial n} = 0$, is also known as the natural boundary condition [40].

The advantage of using scalar potential is that magnetic field is represented by a scalar value rather than a vector having three components. It makes it simpler due to which computation time reduces. But in a case like 3D machine modeling, both Magnetic Scalar and Magnetic Vector potential are used as it is difficult to just use magnetic scalar potential. This is called *mixed formulation*.

5.5 Maxwell's Stress Tensor

In order to have accurate torque values, higher element density is required hence more computation time. For that Maxwell Stress Tensor allow fast calculation of electromagnetic forces acting on the electrical machine. Maxwell stress tensor can work with both scalar and vector magnetic potentials. It is usually calculated over a cylindrical surface in the air-gap of the machine. To calculate electromagnetic torque in the machine, it is written as given in equation 5.21.

$$T_e = \oint_S r \times F' dS \tag{5.21}$$

where $T^{'}$ represents force per unit area. Where $F^{'}$ is given as:

$$F^{'} = \begin{bmatrix} F_{xx} & F_{xy} & F_{xz} \\ F_{yx} & F_{yy} & F_{yz} \\ F_{zx} & F_{zy} & F_{zz} \end{bmatrix}$$

where F_{ij} represents the shear force in **ith** direction pointing towards the **jth** direction on the surface element.

For torque calculation of 3D machines, equation 5.22 can be written as[41]:

$$T_e = \frac{1}{\mu_0} \iint_S r B_r B_\theta dS \tag{5.22}$$

Chapter 6

Finite Element Modelling using COMSOL Multiphysics

Chapter Summary: This chapter explains DR-PMSM finite element modeling in COMSOL. The steps taken to build the 3D FEM model of the machine are discussed. It also explains the results obtained from the simulations and comments on the machine ability to do field weakening.

6.1 Finite Element Modelling

To understand any physical phenomena, we need to arrive at an analytical solution based on differential equations. But the analytical solution of this kind of equations is generally hard to derive. To comprehend these we generally rely on the numerical methods to reach a solution. The Finite Element Method (FEM) is one of the numerical methods used for these kind of problems. Theory of FEM is not explained in detail here. A problem consisting of partial differential equations can be transformed into a simpler system of algebraic and dynamic equations by using FEM, which is then solved by general methods. The geometry on which this system of equations are solved is sub divided into small elements. This set of elements are connected by nodes and are called ”mesh”. The shape of the elements can be of various types such as triangular, tetrahedral or quadrilateral to name a few. The final solution with in the elements are approximated as by interpolating the values of the solution on the nodes. To find the solution on the nodes many methods can be implemented, which results in a linear system of equations. Which can be solved to get our result. The equation is given by,

$$A\vec{u} = b; \tag{6.1}$$

Where **A** is the matrix which is always sparse and often a diagonally dominant matrix, $\vec{u}$ is a vector containing the solutions of all the nodes and **b** is vector linked to the boundary conditions.

6.2 COMSOL Multiphysics

COMSOL Multiphysics is a popular FEM software. It allows the user to concentrate on physics, geometry and results and it performs all the underlying FEM calculations.

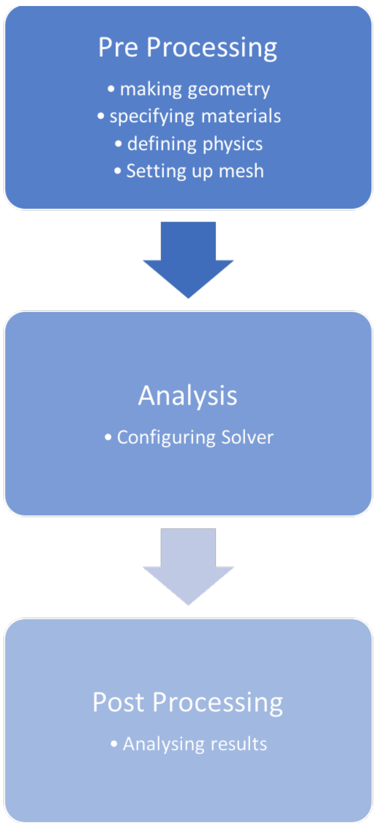

Figure 6.1: Steps for finite elemnet modelling in COMSOL

It can handle various physics such as electromagnetic, acoustics, thermal, electric circuits etc. in a multi physics environment. The user can couple equations from different physics settings. With COMSOL user is able to define the governing equations and initial conditions as per problem. Specific material properties are built in and can be defined as per requirement. For this thesis, Rotating Machinery Magnetic physics module is used for simulations on COMSOL. It allows flexible meshing environment and allows the user to define mesh for any complex geometry as per requirement. There are a variety of solvers as well to choose from. Modeling in COMSOL is a simple 3 step process as shown in figure 6.1. COMSOL Multiphysics Version 5.2a is used in this thesis.

6.3 Machine Modelling in 3D

As discussed earlier, in order to understand the how the dual rotor PMSM behaves, a 3D machine model was to be made. This was compared with a 2D model of a regular PMSM.[42]. In order to model the machine in 3D there were some assumptions made:

6.3.1 Assumptions

1. The material used in the machine model are linear, so that computational time can be reduced.
2. The resistance of the coils has not been modeled.
3. There are eddy current losses considered in the machine stator and for that laminations are modeled as permittivity and conductivity tensor
4. There are no eddy current losses considered in the rotor yoke and magnets.
5. There losses in the machine have not been considered.

6.3.2 Geometry

Finite element models of 3D electrical machines are more difficult to make than 2D models but COMSOL GUI is quite user friendly and offers more flexibility. The 3D finite element model of electrical machine in COMSOL comprises of two rotating parts stator and rotor, which forms an *assembly*. There are different tools which help to obtain the required geometry and there are many ways to achieve it.

In 3D modeling, the first thing to remember is that moving parts are built on individual planes. Usually, stator, stator windings, rotor and magnets are all built on their individual planes. After completing the geometry, rotor and magnets are conformed in a union and similarly stator and windings are conformed in another union.

In order to obtain a 3D stator model, a 2D plane is created and the geometry is built on it; which is extruded in length. While modeling a dual rotor, to achieve the required geometry of the rotor with a gap and movable rotor. Rotor planes were divided into 4 individual planes. The two rotors with magnets are built on separate planes and extruded half the length of the machine. The machine gap between the rotor is modeled on separate two planes and then are merged with their respective rotors with a *union*. Windings were built on a separate plane and merged with the stator to form an assembly.

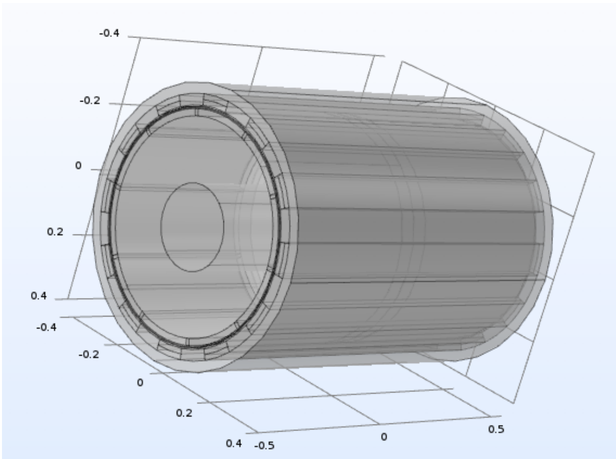

Figure 6.2: Machine geometry

6.3.3 Material Properties

Materials play a vital role in defining physics, differential equations and how the results will end up. COMSOL has many built in materials and helps the user to define its own as well.

The geometry of the dual rotor PMSM demands that the air should be in between the gap of the two rotors and this can be easily specified. Similarly, for magnets, rotor and stator iron and coils materials are specified from the built in material properties from the library.

The material property that is of significance in the model is permeability and conductivity of the material. The rotor yoke permeability is constant and conductivity is assumed to be almost negligible so that computations are less time costly.

The permeability of conductors and airgap is defined as a scalar quantity. For stator iron and rotor yoke, it is not that straightforward. To model lamination, not every sheet can be modeled in 3D. So we take assistance from permeability tensor defined earlier in section 5.2[43].

The stacking factor is taken as 0.95 and the relative permeability for iron is taken as 5000. Also the conductivity tensor is defined to study eddy currents:

$$\mu = \begin{bmatrix} 4750 & 0 & 0 \\ 0 & 4750 & 0 \\ 0 & 0 & 19.3 \end{bmatrix} \sigma = \begin{bmatrix} 1.064e7 & 0 & 0 \\ 0 & 1.064e7 & 0 \\ 0 & 0 & 19.9 \end{bmatrix}$$

6.3.4 Defining Physics

When specifying physics, COMSOL offers various built in features that helps user to implement a model according to requirements.The built in feature that helps in modelling 2D and 3D electrical machines is the *Rotating Machinery, Magnetic* physics node. Special care has to be taken while dealing with both scalar and vector potentials. The rotor, magnets and the airgap is set up with magnetic scalar potential.The stator and the coils are set up with magnetic vector potential and the differential equation dealing with it is as follows:

$$\bigtriangledown \times \left(\frac{1}{\mu} \bigtriangledown \times \vec{A} \right) = \vec{J} \tag{6.2}$$

$$\bigtriangledown^2 \vec{A} = -\mu\sigma(- \bigtriangledown V - \frac{\partial \vec{A}}{\partial t}) \tag{6.3}$$

In the mixed formulation region, the regions of scalar potential are dealt by the following equation, from equations 5.4 and 5.16 we have:

$$- \bigtriangledown \cdot (\mu \bigtriangledown \phi) = 0 \tag{6.4}$$

The magnetic insulation boundary is automatically set, assuming no flux leaves the machine. COMSOL takes care of the Neumann and Dirichlet conditions; one has to specify the scalar and vector potential regions carefully.

For calculating torques and different forces in the machine, *Force Calculation* nodes can be added. As COMSOL uses Maxwell stress tensor for calculating forces[44] then specifying the correct surface is a crucial task. The surface for force calculation node should be inside the *prescribed rotation velocity* boundary surface. For accuracy, rings should be added in the airgap while making the geometry, so the element size can be controlled while meshing. In the machine model, three rings were added in the airgap to have better sliding mesh. These can be seen in zoomed part of the figure 6.3.

6.3.5 Setting up Mesh

By increasing the mesh density solution accuracy is increased by many folds. However, this also requires more degrees of freedom, which demands more memory and more time for computations. This model was meshed by taking into account these concerns.

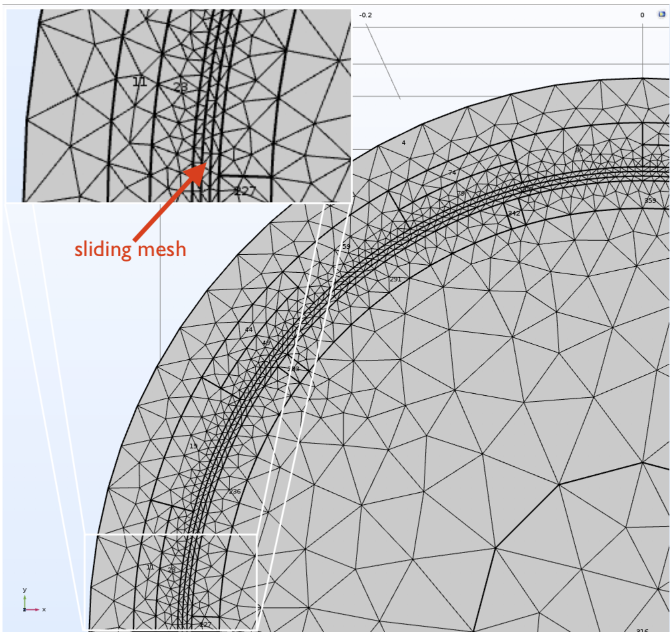

Figure 6.3: Meshing of the machine

The quality of the mesh elements is a clear indicator of the accuracy of the solution. The shape and size of the elements and how they are placed determine the mesh quality. The elements resembling equilateral triangles and rectangles are considered for high quality meshing. The meshing order is also very essential in meshing quality. COMSOL advises to the meshing of the more complex regions first and the simplest region at the end. In electrical machines sliding mesh is given the most importance, as it is used to determine the forces and torques in the machines.

For 2D models, meshing is relatively simpler. For 3D models, with more non-identical planes extruded to make one geometry, makes it more complex. For 3D models *swept mesh* is generally used for geometries where geometry is the same through out the length. A basic check is for applying sept mesh is that objects source and destination faces should match. A free triangular mesh is applied on one face and the rest is swept through out the geometry by swept meshing.

The triangular mesh is applied on one face of the stator, called as source face. Afterwards, a swept mesh is used to sweep the mesh through the entire stator. For two halves of the rotor, which have magnets, the same free triangular mesh is used to mesh the rotor on the source faces and then swept mesh is used to mesh the rotor along the length.

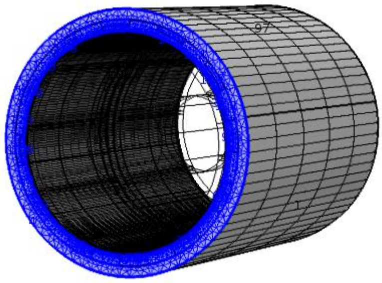

Figure 6.4: Meshing of stator

For the regions in between the rotors which have air and shaft of the rotor, a free tetrahedral mesh is applied on the remaining geometry.
Important point Elements at the destination identity pairs, which should be checked that are towards rotor side of the sliding mesh, can be defined half or even smaller than the size of source identity pairs.

6.3.6 Setting up solvers

Two types of solvers are present in COMSOL to solve the system of linear equations. Depending upon the complexity of the problem particular type of solver should be used [45].

1. **Direct Method**: It uses LU decomposition to solve linear system equations to arrive at a solution The default direct solver of COMSOL is MUMPS and it is used for all the models made in the thesis. The direct solvers require quite a lot of memory but are extremely accurate and converge for linear problems.

2. **Iterative Method**: In this method, the number of unknowns are decreased at every step as initially a guessed solution is added. This requires less memory

and for some 3D models, it is very accurate and faster as compared to direct solvers.

As concluded by W. Frei in [45] "*The direct solvers will use more memory than the iterative solvers, but can be more robust*". The article also points out that COMSOL smartly recognizes the type of solver required for the problem/model.

In this thesis as the 3D model was larger, the iterative method should have been adopted but as the model had both vector and scalar potentials the resultant matrix was not symmetric therefore iterative solvers never converged. Therefore, direct solvers were used for the current problem. For running the machine model, first *stationary study* is used for computing magnetic fields generated by magnets and *time dependent* study solves transient simulations of the PMSM.

6.3.7 Post-Processing

After the simulations are completed, the simulation results are computed by defining variables globally. COMSOL gives a wide variety of plots that can be computed defining area of interest in the geometry. The simulation results are discussed in the later section.

6.4 Results and Observations

The area of interests in the simulation of dual rotor PMSM are:

1. Validity of the machine
2. Effect of forces.
3. Effect of voltages in the coils
4. Flux in the stator iron.

6.4.1 Validity of the machine model

In order to be sure that the modeled machine is generating the right results, it was compared to a conventional PMSM with same parameters by another simulation. If DR-PMSM is in its normal state, where the magnets are not shifted, it should behave as a conventional PMSM. So, a 2D finite element model of conventional PMSM was modeled in COMSOL. Two parameters are of importance to check the validity; induced voltage and power in the machine. The induced voltages of both the machines are compared at no load and loaded conditions. As seen from figure 6.5, the induced voltage is around 1100 V and the terminal voltage is around 1200 V for DR-PMSM. We observe similar voltage levels in 6.6, which shows conventional PMSM's induced and terminal voltages'.

The ripple in the voltages of DR-PMSM simulations is because of a less fine mesh. It could be also because of the harmonics but it was observed that these ripples were reduced by making the mesh finer. The mesh was not made too fine to save computation time consumption.

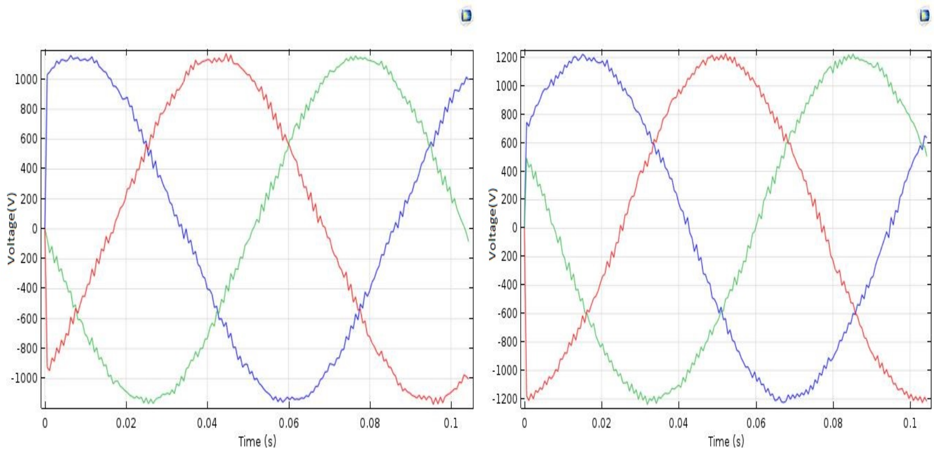

(a) Induced Voltage at no load conditions **(b)** Terminal Voltage at loaded conditions

Figure 6.5: Induced emf and terminal voltage for DR-PMSM

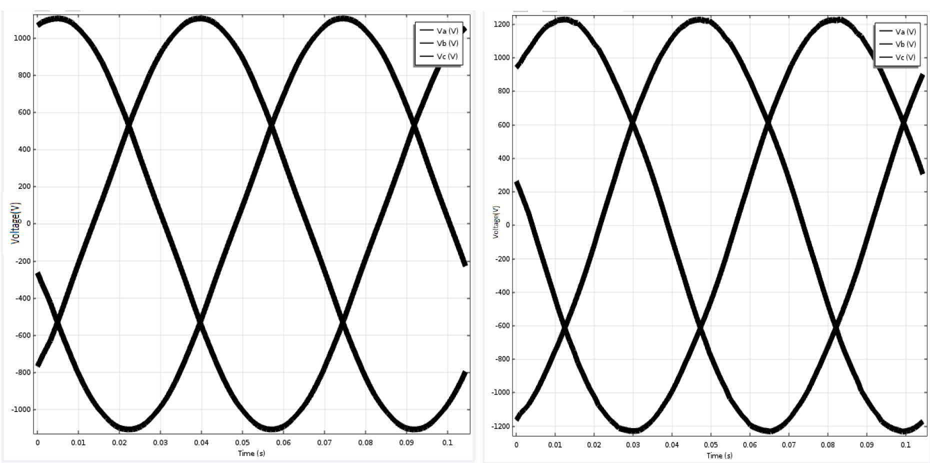

(a) Induced Voltage at no load conditions **(b)** Terminal Voltage at loaded conditions

Figure 6.6: Induced emf and terminal voltage for conventional PMSM

The next thing to be observed is the power in the machine. To confirm the machine model's validity, the power balance in the electrical machine should hold, which is mechanical power must be equal to electrical power[1]. It can be mathematically written as:

$$T_e \omega = V_a I_a + V_b I_b + V_b I_b \tag{6.5}$$

The figure 6.7 shows that mechanical power and electrical power of the DR-PMSM model, both are around .41 MW. This is also true for the conventional PMSM model. It is clear from the simulations, that both the machine models hold the power balance which confirm their validity. As torque is a function of the active length of the machine therefore power produced by DR-PMSM is the same as the conventional PMSM, which confirms the DR-PMSM model is also accurate.

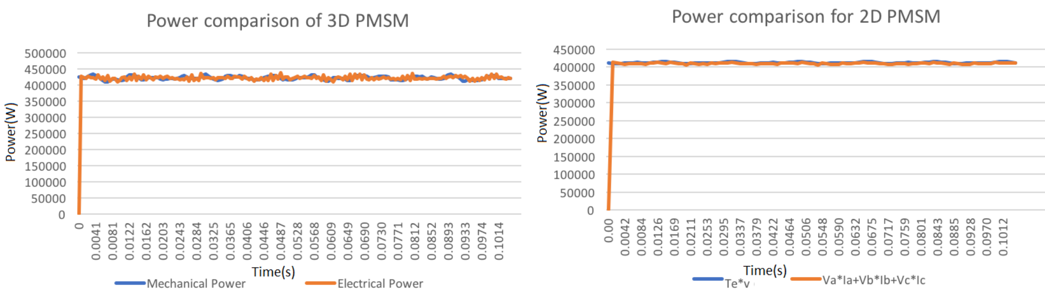

(a) DR-PMSM **(b)** Conventional PMSM

Figure 6.7: Mechanical and Electrical power of the PMSM

6.4.2 Voltages

To confirm that DR-PMSM actually makes the induced voltages to zero by flux weakening, simulations were performed by shifting the magnets by 180 degrees electrically, with no load and loaded conditions.

In figure 6.8a, when the machine is not loaded, the voltages have dropped drastically to a mere 1-2 V. The phasors diagram in figure 6.9a show the DR-PMSM at normal conditions behaves exactly like conventional PMSM. When the machine is shifted by 180 degrees the voltage induced goes to zero as expected as shown in figure 6.9b. The phasors show that the only voltage that remains in the machine is due to the currents in the stator windings which can also be seen in figure 6.8b.

[1]Ignoring the machine losses, as they are not modeled

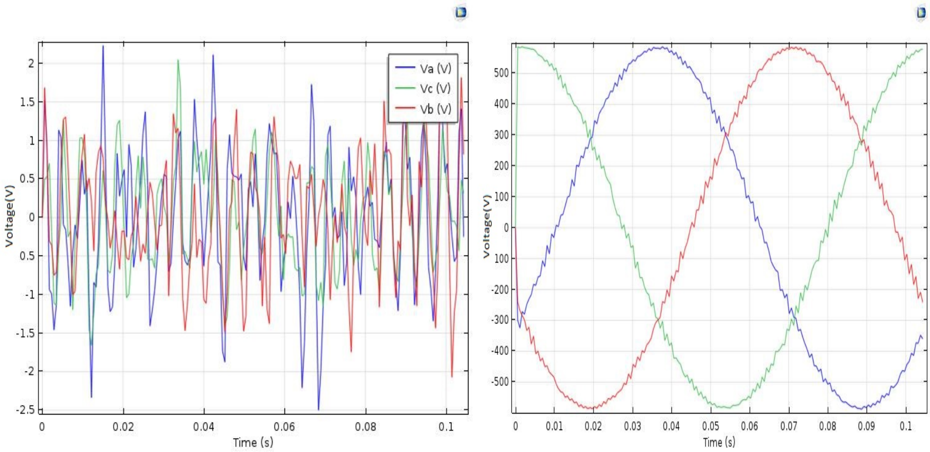

(a) Induced Voltage at no load conditions **(b)** Terminal Voltage at loaded conditions

Figure 6.8: Induced emf and terminal voltage at 180 degrees

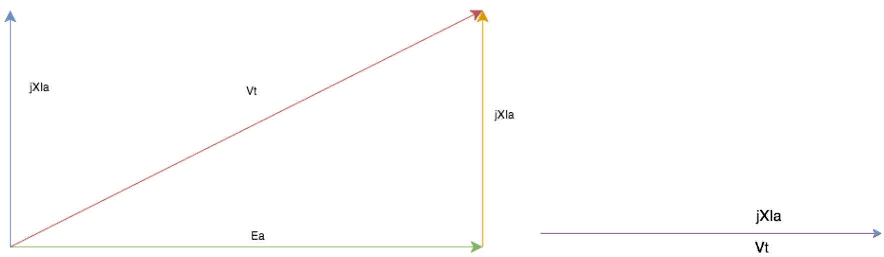

(a) Magnets shifted by 0 degrees **(b)** Magnets shifted by 180 degrees

Figure 6.9: Phasor Diagram : Terminal voltage, induced emf and current for phase A

To observe the effect on voltage by field weakening in DR-PMSM, a simulation was carried out at different rotor positions and maximum voltages were computed. The voltages at 0 mechanical degrees is 1150 V and the voltage at 36 mechanical degrees is almost 0 V. The reduction of voltages by flux weakening can be observed clearly in the plot between various rotor position and maximum voltages in figure 6.10.

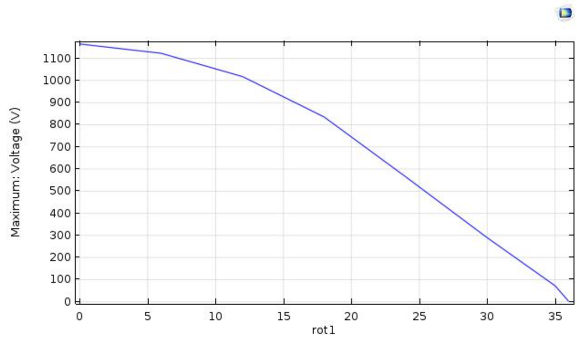

Figure 6.10: Voltage in phase A at various rotor positions

It can be easily concluded that DR-PMSM has the ability to completely reduce the flux to zero by field weakening.

6.4.3 Forces

The Force calculation nodes were set up on both the rotors and axial forces were calculated using Maxwell stress tensor. To understand how the forces interact, rotor 1 is shown in the figure 6.11 with the z-axis.

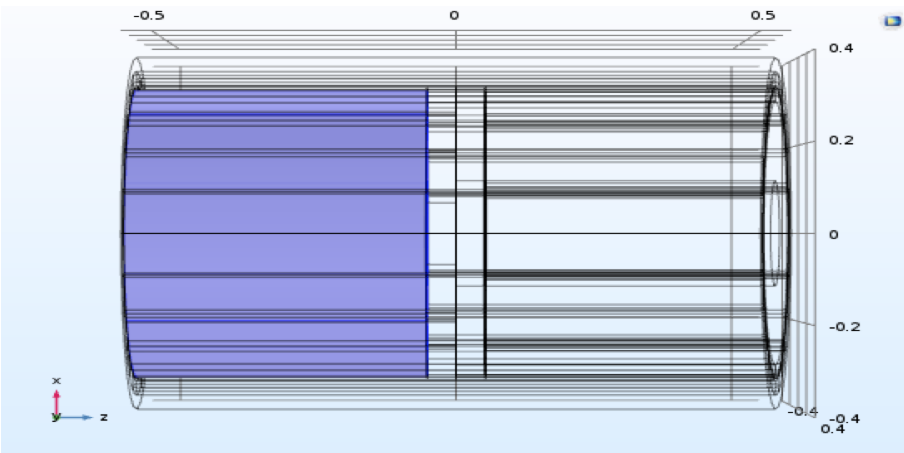

Figure 6.11: Rotor 1 is selected, top view of the PMSM

The forces acting upon the two rotors are dealt in two cases; with no load case and with rated currents in the coils case.

Case 1: No load case

The figure 6.12 shows the forces on the rotors and the cogging torque produced at no load when the magnets are electrically shifted by 0 and 180 degrees. The figure 6.12a shows that the two rotors repel each other by equivalent forces of 300 N and figure 6.12b shows that equivalent amount of attractive forces of 2500 N, are present when magnets are 180 degrees shifted. Also, the red curve defines the high cogging torque in the machine, even when the rotors are misaligned we observe the similar amount of cogging torque.

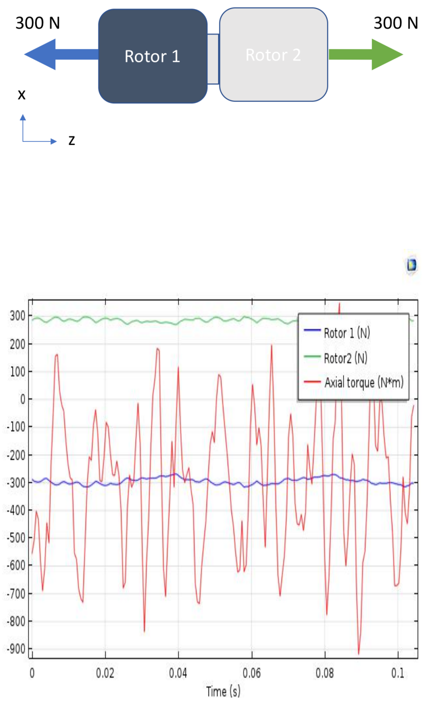

(a) Magnets shifted by 0 degree

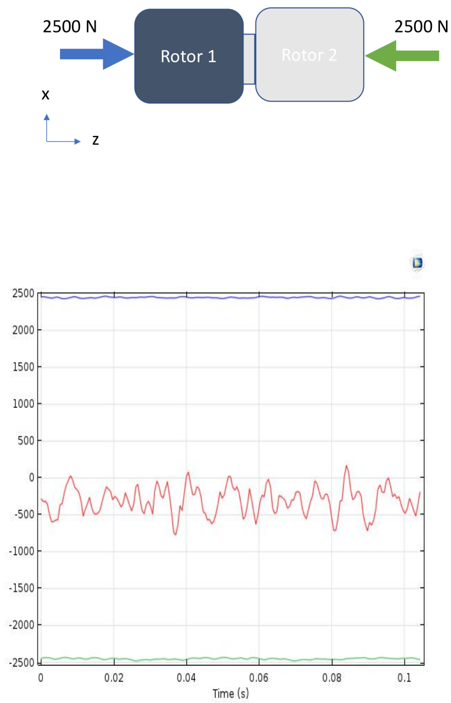

(b) Magnets shifted by 180 degrees

Figure 6.12: Axial forces on rotors and Torque at no load

Case 2: Loaded case

Similarly, in the case where there is current in the conductors, it can be seen in figure 6.13a that the forces magnitude increase to 1800 N and the two rotors repel each other. The red line indicates that torque in the machine which is around 35kNm. Also, in the case of 180 degrees shifted magnets, it can be seen in figure 6.13b that the two rotors attract each other with a higher magnitude of forces. These forces that repel each other are not equal because of the currents in the windings.

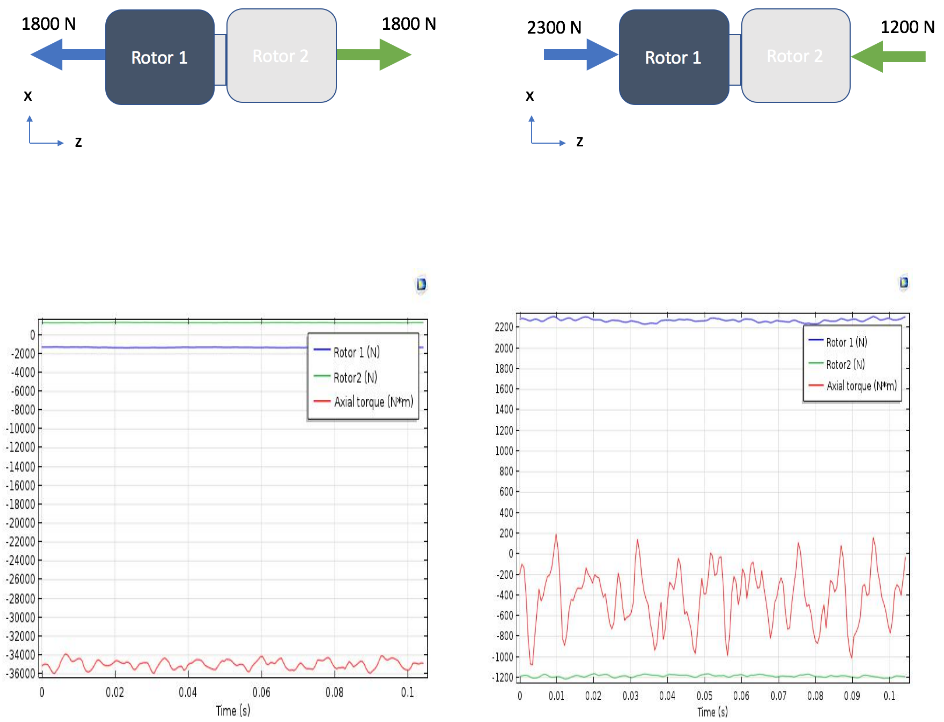

(a) Magnets shifted by 0 degrees **(b)** Magnets shifted by 180 degrees

Figure 6.13: Axial forces on rotors and Torque at loaded conditions

It has been observed that there are attractive and repulsive forces between the two rotors, which makes it crucial to understand the forces on the rotors for the shifting mechanism. For this, a different set of simulation was carried out on a standstill rotor.

Torques on a standstill rotor

In this simulation, axial torques were calculated on the individual rotors while one of the rotors were shifted from 0-360 degrees electrically in a no load, stationary conditions while the other rotor is at standstill.

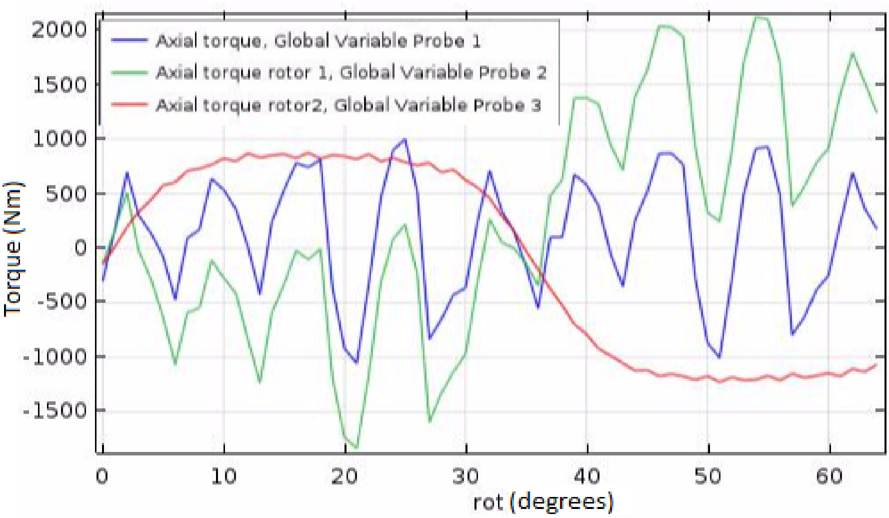

Figure 6.14: Axial torques on rotors

In the figure 6.14, the blue line shows the torque on the stator when one of the rotor is moved 360 degrees. As expected, we observe the cogging in the machine due to stator slot teeth and the poles. The red line describes the forces experienced by the standstill rotor. As seen in the figure the red curve is not experiencing any cogging torque, only forces affecting it are from the adjacent rotor due to change in magnetic fields by misalignment of the magnets. While the green line represents the forces on the moving rotor which clearly has both cogging and the forces acting on from the adjacent rotor.

After analyzing the torques in figure 6.14, it can be concluded that if machine cogging is reduced the forces on the moving rotor can be reduced drastically.

6.4.4 Flux in the stator

The DR-PMSM's construction enables it to control flux by the movement of one of the rotors by misaligning the magnets. This makes the flux an important topic of discussion. In a normal situation, when magnets are not misaligned, the majority of the flux passes through the stator radially. The laminations in the machine are modeled by the help of permeability and conductivity tensors. This makes the machine robust against eddy current losses. The machine radial airgap flux density B_r is observed in figure 6.15. The dips on the peaks of the wave form are because of the stator teeth. The flux lines are more concentrated on the edge of stator teeth and they are less concentrated in between. The basic fundamental of the B_r wave can be seen with stator teeth patterns on the peeks.

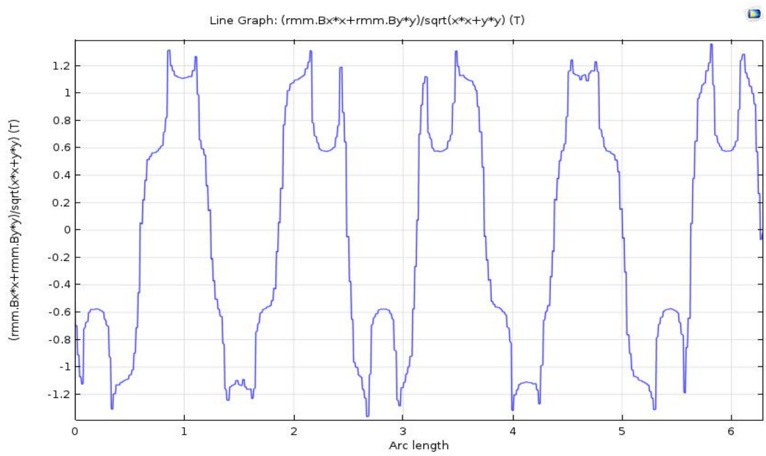

Figure 6.15: Airgap flux density of the machine on Rotor 1

The behaviour of the airgap flux is normal as explained above when magnets are not misaligned. The flux in the axial direction becomes a problem when the magnets are misaligned by 180 degrees and rotated. The flux will tend to pass from north pole to south pole and during that flux in the middle region (figure 6.16) of the stator can pass orthogonally to the laminations. This will induce eddy currents in the stator iron as explained in the appendix. All the analysis are done in the middle of the stator because the flux in the axial direction is concentrated in that region.

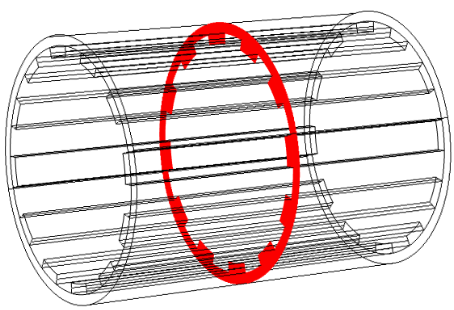

Figure 6.16: Area of interest: middle region of stator

Initially, when magnets are misaligned by 180 degrees the flux is concentrated in the middle part of the stator as shown in figure 6.17a. Later, as the two rotors are allowed to rotate for 57.4 milliseconds, the change in axial flux and formation of eddy currents can be observed in figure 6.17b.

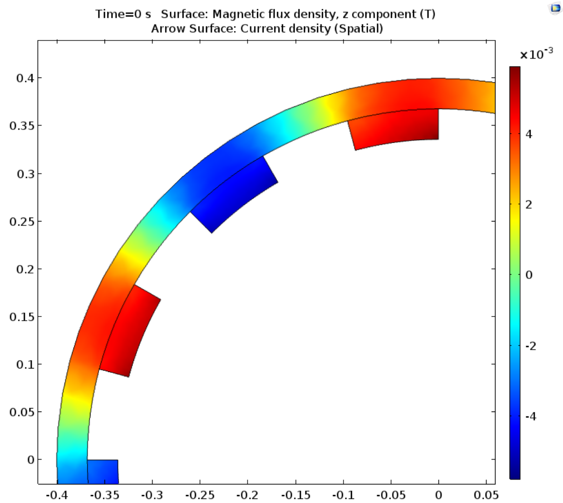

(a) ***Bz***, in the middle of the stator at stationary, stand still conditions

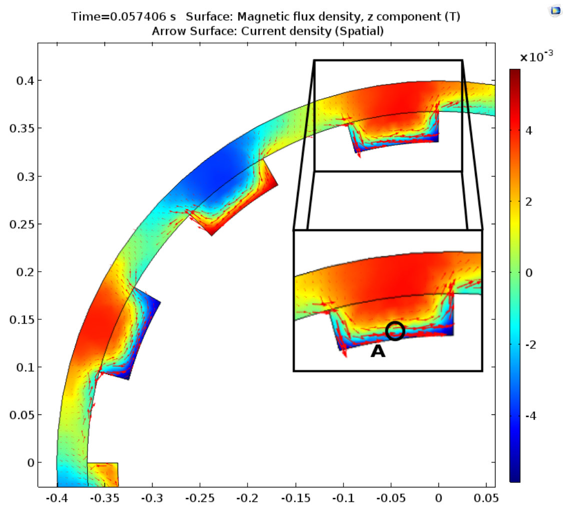

(b) ***Bz***, in the middle of the stator at 57.4 ms

Figure 6.17: Axial magnetic flux density, ***Bz***, in the middle of the stator

The first thing to observe is where the magnetic flux density (***Bz***) is concentrated mostly and how it changes with time. Secondly the induced eddy currents, depicted by the arrows, opposing the change in ***Bz***. The surface plot of (***Bz***), in zoomed part of the figure 6.17b, shows that most ***Bz*** is concentrated in the tooth of the stator. This plot is taken at a time instant of 0.057406 s and the thing to be observed is the region **A** of have high ***Bz*** as marked in figure 6.17b.

To understand how ***Bz*** changes with time, a simulation for a complete mechanical rotation was performed. The change in ***Bz*** at point A can be observed in figure 6.18. The axial flux density keeps varying with time as the two rotors complete the full mechanical rotation. The point in the debate is that this change in flux will induce currents in the stator iron, making the tip of the stator teeth vulnerable to eddy current losses.

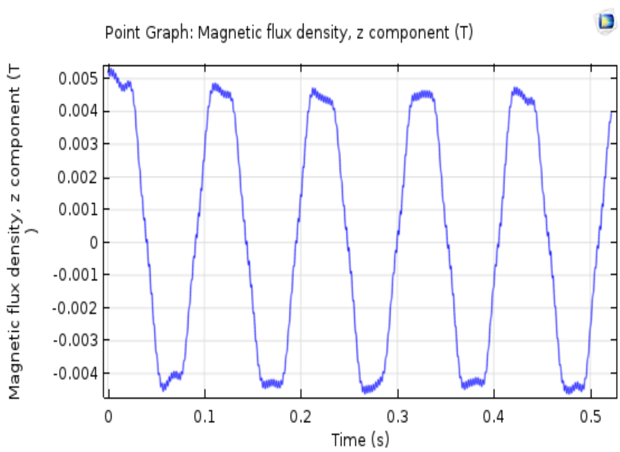

Figure 6.18: Change in ***Bz*** as observed on a point A on stator teeth

To observe the eddy currents flow, a surface current density norm plot at time instant 0.52174s has been taken in the figure 6.19. This shows the currents are mostly concentrated around the edge of the stator teeth and the magnitude of the current is not that large in other parts. The direction of currents and flow is quite visible from the plot. The maximum magnitude of the current is around 40 A/mm^2 which is just concentrated on the edges of the stator teeth.

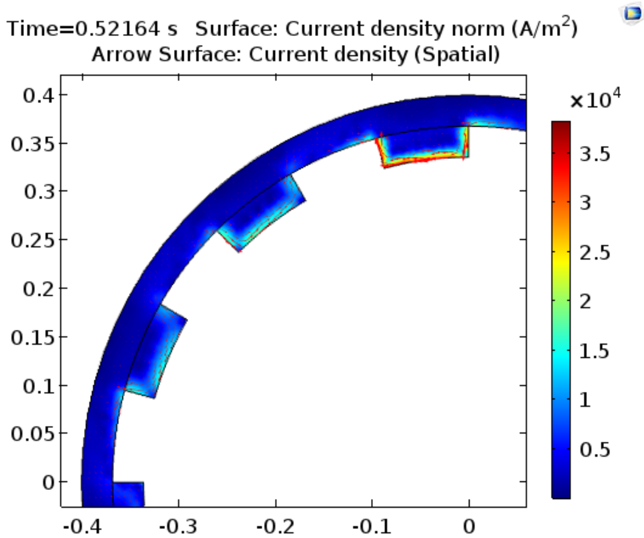

Figure 6.19: Change in direction of current w.r.t. current density norm

The analysis shows that the middle part of the stator iron which is between the two rotors has some eddy current losses. To avoid these losses, a stator with a gap can be made for this particular machine. The windings are continuous but a spacer, having material of zero relative permeability, in the middle part of the stator should be introduced in the design. One can not conclude the severity of these losses from these simulations but the phenomenon of eddy current can be clearly observed in the misaligned machine and needs more research.

Chapter 7

Machine Prototype and Experiments

Chapter Summary: After successful simulations, a practical test was devised to test the theory of the DR-PMSM. This chapter explains the construction of the machine prototype, instrumentation used and the results of the conducted experiments.

7.1 Introduction

To test the theory of field weakening on DR-PMSM, a test was devised. To make a full scale model of the machine was unnecessary and time consuming because the goal here is to validate the theory of field weakening in a DR-PMSM. So, a smaller prototype of the dual rotor PMSM was made by modifying already available PMSM generator. The machine used was an experimental generator used for lab experiments. The old setup was built to teach students about winding layouts and the machine itself does not generate significant power. The students can use wire connectors to design different winding layouts. The generator is connected to an electrical motor by means of a shaft and controlled by a frequency converter.

7.2 New prototype

The new prototype used the old stator of 170 mm inner diameter and new split rotor was constructed for it with shifting mechanism as shown in figure 7.2b. The

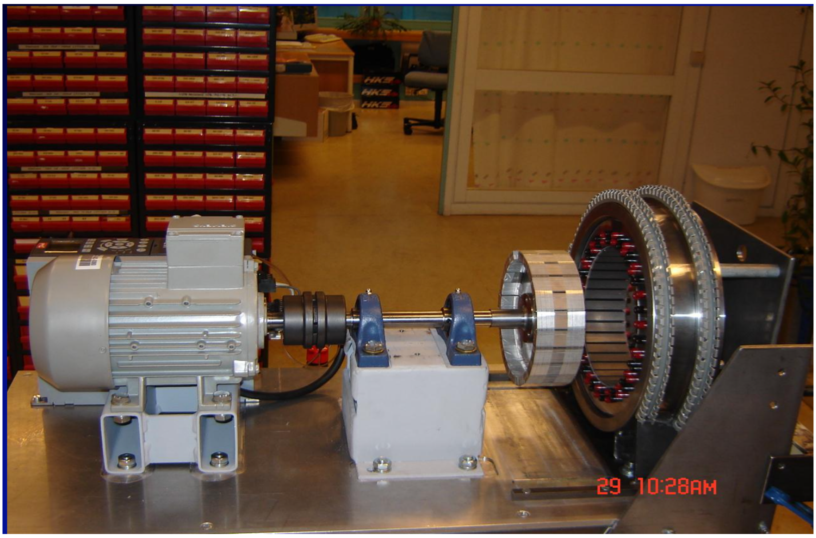

Figure 7.1: The PMSM setup

shifting mechanism is quite simple and enables the angular alignment of the two rotors. The parameters of the machine are as follows:

Table 7.1: Machine Parameters for the DR-PMSM prototype

Parameter	Unit	Value
Machine Diameter	mm	270
Machine active length	mm	48.7
Machine length	mm	50
Rotor radius	mm	157.7
Airgap length	mm	8.3
Rotational Speed	rpm	350
Poles	-	24
Stator slots	-	36
Winding layout	-	Double layer
Magnet length	mm	4

Here $q = \frac{1}{2}$, which implies that concentrated winding should be used as explained in the section 2.5. Double layer windings were used in this machine and the winding layout is shown in figure 7.3.

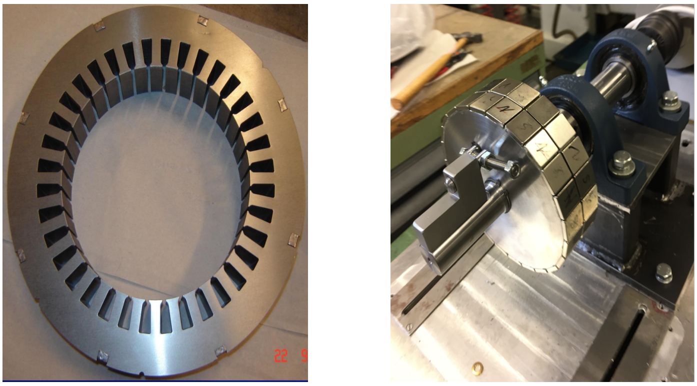

(a) Stator construction **(b)** Rotor Construction

Figure 7.2: Stator and the rotor of the dual rotor machine

Slot #	1	2	3	4	5	6	7	8	9	10	11	12	13	14	15	16	17	18
Phase R	R			R			R			R			R			R		
Phase S		S			S			S			S			S			S	
Phase T			T			T			T			T			T			T
RST	R	S	T	R	S	T	R	S	T	R	S	T	R	S	T	R	S	T
Bottom	-T	-R	-S	-T	-R	-S	-T	-R	-S	-T	-R	-S	-T	-R	-S	-T	-R	-S
SingleP																		

Slot #	19	20	21	22	23	24	25	26	27	28	29	30	31	32	33	34	35	36
Phase R	R			R			R			R			R			R		
Phase S		S			S			S			S			S			S	
Phase T			T			T			T			T			T			T
RST	R	S	T	R	S	T	R	S	T	R	S	T	R	S	T	R	S	T
Bottom	-T	-R	-S	-T	-R	-S	-T	-R	-S	-T	-R	-S	-T	-R	-S	-T	-R	-S
SingleP																		

Figure 7.3: Winding layout of 36 slot 18 pole for DR-PMSM

7.3 Setup

The DR-PMSM was run using an induction motor connected by a shaft. The frequency converter was used to run the machine at 350 rpm. The winding layout was made by connecting wires using the winding layout presented in figure 7.3. Each coils has only one turn as it is just one connecting wire. After setting the alignment of the two rotors using the shifting mechanism, voltage of one coil was measured using oscilloscope. The connection diagram in the figure 7.4 shows the simple setup.

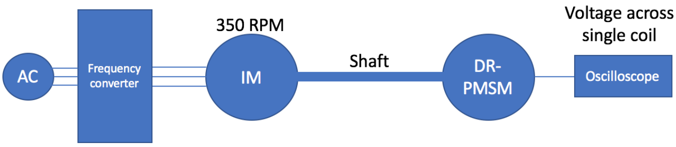

Figure 7.4: Connection diagram

7.4 Experiments

To check how the voltage behaves in the windings by changing the magnetic field. Voltage was measured while shifting the magnets from 0 to 180 degrees and it was expected to decrease with the decrease in magnetic flux. As the windings are made of just one connecting wire, there are harmonics in the voltages and these were expected. Every measurement was taken by changing the angular alignment of the two rotors first at a stand still, then running the generator at 350 rpm by using a frequency converter. As the setup was simple, voltages were just measured across one of the windings by the use of an oscilloscope. The Peak-peak voltage was measured and the results are shown in the figure below:

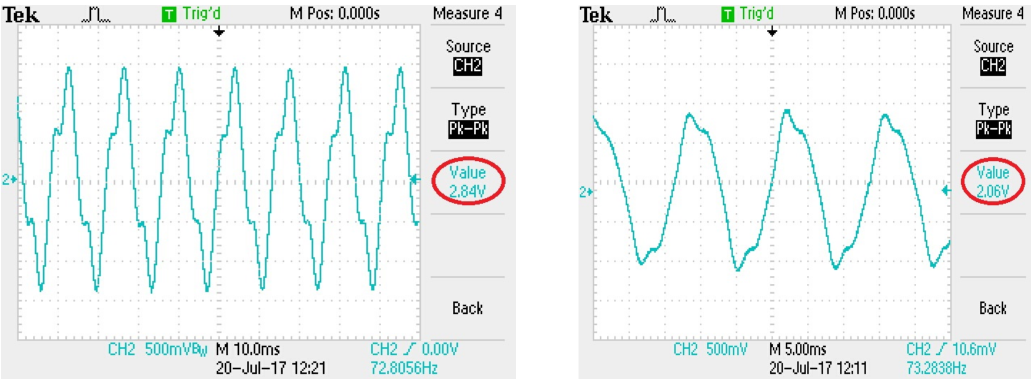

(a) North-north poles aligned at 0 degrees

(b) North-south poles unaligned

Figure 7.5: Voltages on one coil while shifting of magnets from 0 degrees on wards

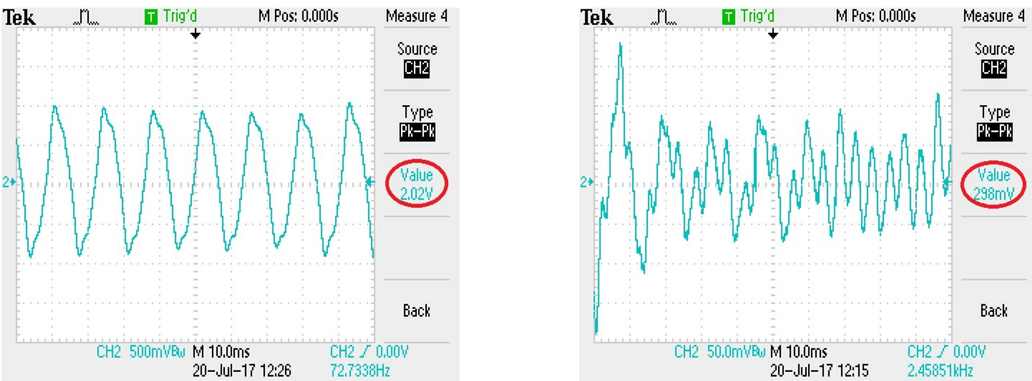

(a) North-south poles unaligned

(b) South-north poles aligned at 180 degrees

Figure 7.6: Voltages on one coil while shifting of magnets to 180 degrees

7.5 Results

The figure 7.5a shows voltage at normal state when the magnets are aligned at 0 degrees. The peak to peak voltage here is 2.84 V, which is the maximum this machine can produce. The figure 7.5b and figure 7.6a shows the voltages when the magnets are slightly misaligned. The voltages are 2.06 V and 2.02V respectively. The last figure 7.6b displays peak to peak voltage when the magnets are shifted 180 degrees and opposite magnets are aligned. The voltage is 298 mV.
It can be seen from the figures 7.5 and 7.6 that voltages drop 2.84 V to 298 mV, just by shifting the magnets. The voltages obtained from the machine are not perfectly sinusoidal because of human errors in the construction of the machine. However, the phenomenon of flux weakening is observed here and this confirms our hypothesis that DR-PMSM is capable of flux weakening. Building the machine prototype gave an overall understanding of the machine and after positive results, it can be concluded that this machine can be practically implemented.

Chapter 8

Conclusions and Future Work

Chapter Summary: This chapter concludes the contributions from this thesis and presents what type of research should be done in future.

8.1 Conclusion

The electromechanical faults, like stator internal faults, are the most common in electrical machines. Offshore applications are more vulnerable to stator winding faults because of insulation degradation due to high temperatures and the environmental conditions. These faults are hazardous and if not stopped can lead to a fire on the Wind turbines or the shaft generators of marine applications. Flux weakening by using DR-PMSM is the way suggested to solve internal stator faults in WTs and marine applications so that generators are not shut down or propulsion should not be stopped.

After 3D FEM modeling of DR-PMSM following conclusions were drawn from simulation results and experiments on the machine prototype.

1. It is equally power efficient as a conventional PMSM and torque is the function of the active length of the machine.

2. Induced voltages can be reduced to zero by flux weakening mechanism in DR-PMSM.

3. The forces on rotors due to shifting mechanism can be minimized by reducing cogging in the machine.

4. Due to shifting mechanism axial flux component in the machine induces certain hot spots in the middle part of the stator (between the gap of the two rotors), which should be further studied.

5. The machine prototype confirms the theory of flux weakening in DR-PMSM and validates the practicality of this machine.

For the shaft generator of marine propulsion drive train, the R2 type redundancy by DNVGL can be met using this DR-PMSM. As it will make the machine electrically dead by flux weakening. If an efficient gear mechanism is built for shifting the magnets then the machine can be made electrically dead in matter of minutes making it the most efficient solution in the market.

For wind turbines DR-PMSM can be used for field weakening and can avoid complete shut down of the generators. They require better power electronics to control the power output of the generator. The idea requires more research and this thesis leaves this topic open.

8.2 Contributions

1. A 3D transient finite element model of DR- PMSM was built. That can be used to model generally any electrical machine.

    - The model was able to comment on the effect of forces between the two rotors.
    - The model was able to point out possible hot spots in the middle region of the stator.

2. A 2D model of conventional PMSM was made to compare it with 3D model of DR-PMSM. The model confirms that DR-PMSM is equally power efficient as a conventional PMSM.

3. The test on machine prototypes confirms the practicality of the DR-PMSM and flux weakening capabilities.

8.3 Future Work

1. Internal fault conditions: Fault currents can be introduced in the windings to study how they behave with flux weakening can be studied.

2. Forces: The forces on the two rotors should be studied as a function of the gap between two rotors.

3. Industrialization: Design work focusing on mechanical and magnetic design should be done with the industry.

4. Thermal design: loss analysis of eddy current in a more practical design to be done.

5. Alternative methods: more methods should be researched to implement field weakening in the machine.

Bibliography

[1] Ronald Dean Bremner. Dual rotor electromagnetic machine, August 18 2009. US Patent 7,576,465.

[2] Øystein Krøvel. Design of large permanent magnetized synchronous electric machines. *Doctoral Theses, Norwegian University of Science and Technology, Norway*, 2011.

[3] Jin-Hyung Yoo and Tae-Uk Jung. Fault diagnosis method of permanent magnet synchronous motor for electrical vehicle. *Journal of Magnetics*, 21(3):413–420, 2016.

[4] M Van der Geest. *Design and Modeling of High Performance Permanent Magnet Synchronous Machines*. PhD thesis, TU Delft, Delft University of Technology, 2015.

[5] Faeture news. How two mechanics who got caught by a wind turbine fire helped the wind industry. `https://www.gineersnow.com/industries/renewables/two-mechanics-died-wind-turbine-fire-helped-wind-industry`. Accessed: 2017-04-015.

[6] John S Hsu. A machine approach for field weakening of permanent-magnet motors. Technical report, SAE Technical Paper, 2000.

[7] TA Lipo and M Aydin. Field weakening of permanent magnet machines–design approaches. In *EPE Power Electronics and Motion Control Conference (EPE-PEMC 04)*, 2004.

[8] BJ Chalmers, R Akmeşe, and L Musaba. Design and field-weakening performance of permanent-magnet/reluctance motor with two-part rotor. *IEE Proceedings-Electric Power Applications*, 145(2):133–139, 1998.

[9] Longya Xu, Lurong Ye, Li Zhen, and Ahmed El-Antably. A new design concept of permanent magnet machine for flux weakening operation. *IEEE Transactions on Industry Applications*, 31(2):373–378, 1995.

[10] Juan A Tapia, Franco Leonardi, and Thomas A Lipo. Consequent-pole permanent-magnet machine with extended field-weakening capability. *IEEE Transactions on Industry Applications*, 39(6):1704–1709, 2003.

[11] Kim Houng Joong, Kazuo Tahara, Kou Ajima, Koki Ueta, Toshiyuki Innami, Noriaki Hino, Taizo Miyazaki, Tomoyuki Hanyu, Kousaku Ohno, et al. Hybrid car and dynamo-electric machine, June 10 2003. US Patent 6,577,022.

[12] Duane C Hanselman. *Brushless permanent magnet motor design*. The Writers' Collective, 2003.

[13] Ø Krøvel, R Nilssen, and A Nysveen. A study of the research activity in the nordic countries on large permanent magnet synchronous machines. *NORPIE 2004*, 2004.

[14] Z Daneshi-Far, GA Capolino, and H Henao. Review of failures and condition monitoring in wind turbine generators. In *Electrical Machines (ICEM), 2010 XIX International Conference on*, pages 1–6. IEEE, 2010.

[15] Olav Vaag Thorsen and Magnus Dalva. A survey of faults on induction motors in offshore oil industry, petrochemical industry, gas terminals, and oil refineries. *IEEE transactions on industry applications*, 31(5):1186–1196, 1995.

[16] Dionysios V Spyropoulos and Epaminondas D Mitronikas. A review on the faults of electric machines used in electric ships. *Advances in Power Electronics*, 2013, 2013.

[17] Vinko Lešic, Mario Vašak, Goran Stojcic, and Thomas M Wolbank. Fault-tolerant control of permanent magnet synchronous generator in wind turbines. *European Wind Energy Association 2014 Annual Event, EWEA*, page 6, 2014.

[18] Szilard Jagasics and Istvan Vajda. Comparison of different pmsm rotor configurations. In *Electric Vehicle Conference (IEVC), 2014 IEEE International*, pages 1–5. IEEE, 2014.

[19] Juha Pyrhonen, Tapani Jokinen, and Valeria Hrabovcova. *Design of rotating electrical machines*. John Wiley & Sons, 2009.

[20] SE Skaar, O Krovel, and R Nilssen. Distribution, coil-span and winding factors for pm machines with concentrated windings. *ICEM 2006*, pages 2–5, 2006.

[21] Ayman M El-Refaie and Thomas M Jahns. Optimal flux weakening in surface pm machines using fractional-slot concentrated windings. *IEEE Transactions on Industry Applications*, 41(3):790–800, 2005.

[22] Astrid Røkke. Permanent magnet generators for marine current tidal turbines. 2017.

[23] Arun Gandhi, Timothy Corrigan, and Leila Parsa. Recent advances in modeling and online detection of stator interturn faults in electrical motors. *IEEE Transactions on Industrial Electronics*, 58(5):1564–1575, 2011.

[24] Lars Henrik Hansen, Lars Helle, Frede Blaabjerg, E Ritchie, Stig Munk-Nielsen, Henrik W Bindner, Poul Ejnar Sørensen, and Birgitte Bak-Jensen. Conceptual survey of generators and power electronics for wind turbines. Technical report, 2002.

[25] Kevin Alewine and William Chen. A review of electrical winding failures in wind turbine generators. *IEEE Electrical Insulation Magazine*, 28(4), 2012.

[26] DNV GL AS. Rules for classifications: Ships-dnvgl-ru-ships pt.4 ch.8 edition jan 2017. Technical report, 2017.

[27] Brent S Gagas, Kensuke Sasaki, Takashi Fukushige, Apoorva Athavale, Takashi Kato, and Robert D Lorenz. Analysis of magnetizing trajectories for variable flux pm synchronous machines considering voltage, high-speed capability, torque ripple, and time duration. *IEEE Transactions on Industry Applications*, 52(5):4029–4038, 2016.

[28] Dong-Kyun Woo and Byung Hwan Jeong. Irreversible demagnetization of permanent magnet in a surface-mounted permanent magnet motor with overhang structure. *IEEE Transactions on Magnetics*, 52(4):1–6, 2016.

[29] Andrew Shakal, Yuefeng Liao, and Thomas A Lipo. A permanent magnet ac machine structure with true field weakening capability. In *Industrial Electronics, 1993. Conference Proceedings, ISIE'93-Budapest., IEEE International Symposium on*, pages 19–24. IEEE, 1993.

[30] Thomas A Lipo, Yuefeng Liao, and Feng Liang. Field weakening for a doubly salient motor with stator permanent magnets, October 3 1995. US Patent 5,455,473.

[31] Brian J Chalmers, Lawrence Musaba, and David F Gosden. Variable-frequency synchronous motor drives for electric vehicles. *IEEE transactions on industry applications*, 32(4):896–903, 1996.

[32] Lawrence P Zepp and Jerry W Medlin. Brushless permanent magnet motor with variable axial rotor/stator alignment to increase speed capability, December 10 2002. US Patent 6,492,753.

[33] Masahiro Masuzawa, Noriyoshi Hirao, Takashi Sasaki, and Masahiro Mita. Brushless motor having permanent magnets, October 13 1998. US Patent 5,821,710.

[34] Kim Houng Joong and Shigeta Ueda. Dynamo-electric machine having a rotor with first and second axially or rotationally displaceable field magnets, December 13 2005. US Patent 6,975,055.

[35] Kim Houng Joong, Kazuo Tahara, Kou Ajima, Koki Ueta, Toshiyuki Innami, Noriaki Hino, Taizo Miyazaki, Tomoyuki Hanyu, Kousaku Ohno, et al. Hybrid car and dynamo-electric machine, October 8 2002. US Patent 6,462,430.

[36] Houng Joong Kim and Shigeta Ueda. Wind power generation system, April 1 2003. US Patent 6,541,877.

[37] Nicola Bianchi. *Electrical machine analysis using finite elements*. CRC press, 2005.

[38] Johannes Ziske, Holger Neubert, and Rolf Disselnkötter. Modeling of anisotropic laminated magnetic cores using homogenization approaches. 2014.

[39] FM Wani. Three dimensional finite element modeling of a brushless doubly-fed induction machine. 2016.

[40] Sheppard Joel Salon. *Finite element analysis of electrical machines*, volume 101. Kluwer academic publishers Boston USA, 1995.

[41] KJ Meessen, JJH Paulides, and EA Lomonova. Force calculations in 3-d cylindrical structures using fourier analysis and the maxwell stress tensor. *IEEE Transactions on Magnetics*, 49(1):536–545, 2013.

[42] Nirmal Paudel. Important steps for modeling a 3d rotating machine. `https://www.comsol.com/blogs/guidelines-for-modeling-rotating-machines-in-3d/`. Accessed: 2016-12-18.

[43] CJ Carpenter. Theory of flux penetration into laminated iron and associated losses. In *Proceedings of the Institution of Electrical Engineers*, volume 124, pages 659–664. IET, 1977.

[44] Oliver Vogel and Jürgen Ulm. Theory of proportional solenoids and magnetic force calculation using comsol multiphysics. In *Proceedings of the 2011 COMSOL Conference in Stuttgart*, 2011.

[45] Walter Frei. Solutions to linear systems of equations: Direct and iterative solvers. `https://www.comsol.com/blogs/solutions-linear-systems-equations-direct-iterative-solvers/`. Accessed: 2017-02-02.

[46] Winncy Y Du. *Resistive, capacitive, inductive, and magnetic sensor technologies*. CRC Press, 2014.

Appendix

Eddy-current losses

The circulating currents induced in the conductors by changing magnetic fields are known as eddy currents. These currents gives rise to unwanted heating in the conductor and give unnecessary power losses. In electrical machines, AC coils give rise to eddy current losses in the stator and iron core. In PM machines radial flux emitted by magnets can cause serious eddy current losses. If the core is made up of single piece of iron then the eddy currents will circulate through out the iron and give rise to huge losses. This problem is simply solved by lowering the reluctance of the core and stator. For that specific reason the machines are stacked with iron sheets and have laminations between them thus lowering the reluctance, because the sheets are thin, the currents are much smaller and they add up to give less losses. The figure 8.1 shows how the currents are induced.

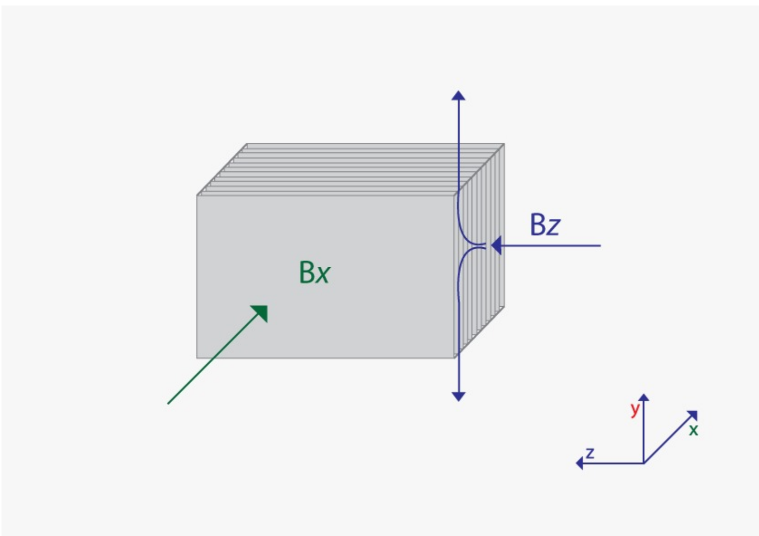

Figure 8.1: Eddy currents in laminated core

Eddy currents losses are proportional to the square of the frequency and magnetic flux density [46]. Hysterisis losses, excess losses and eddy current losses add up to give iron losses. Generally, the iron sheet manufacturers provide value of iron losses in watts for given value of frequency and magnetic fields and the machine designer cater these values while designing the machine [46].